High-Altitude Wind Prediction and Measurement Technology Assessment

30 June 2009

Richard L. Walterscheid
Space Sciences Department
Space Science Applications Laboratory

Prepared for:

Volpe National Transportation Systems Center
U.S. Department of Transportation
Cambridge, Massachusetts

Contract No.: DTRT57-05-D-30103, Task 19

Authorized by: Space Systems Group

AEROSPACE
Assuring Space Mission Success

REPORT DOCUMENTATION PAGE				*Form Approved* *OMB No. 0704-0188*
The public reporting burden for this collection of information is estimated to average 1 hour per response, including the time for reviewing instructions, searching existing data sources, gathering and maintaining the data needed, and completing and reviewing the collection of information. Send comments regarding this burden estimate or any other aspect of this collection of information, including suggestions for reducing the burden, to the Department of Defense. Executive Services and Communications Directorate (0704-0188). Respondents should be aware that notwithstanding any other provision of law, no person shall be subject to any penalty for failing to comply with a collection of information if it does not display a currently valid OMP control number. **PLEASE DO NOT RETURN YOUR FORM TO THE ABOVE ORGANIZATION.**				

1. REPORT DATE (DD-MM-YYYY) 30-06-2009	**2. REPORT TYPE** Contractor Final Report	**3. DATES COVERED (FROM - TO)** April 24, 2008 – May 29, 2009		
4. TITLE AND SUBTITLE High-Altitude Wind Prediction and Measurement Technology Assessment		**5A. CONTRACT NUMBER** DTRT57-05-D-30103		
		5B. GRANT NUMBER		
		5C. PROGRAM ELEMENT NUMBER		
6. AUTHOR(S)* R. L. Walterscheid		**5D. PROJECT NUMBER** FA2R DL411		
		5E. TASK NUMBER Task Order #19		
		5F. WORK UNIT NUMBER FA2R DL411		
7. PERFORMING ORGANIZATION NAME(S) AND ADDRESS(ES) U.S. Department of Transportation Research and Innovative Technology Administration Volpe National Transportation Systems Center Safety Information Systems Division Cambridge, MA 02142-1093		**8. PERFORMING ORGANIZATION REPORT NUMBER** DOT-VNTSC-FAA-09-13		
9. SPONSORING/MONITORING AGENCY NAME(S) AND ADDRESS(ES) U.S. Department of Transportation Federal Aviation Administration Office of the Assoc. Administrator for Commercial Space Transportation Washington, DC 20591		**10. SPONSOR/MONITOR'S ACRONYM(S)** FAA AST-300		
		11. SPONSOR/MONITOR'S REPORT NUMBER(S)		
12. DISTRIBUTION/AVAILABILITY STATEMENT PUBLIC RELEASE IS AUTHORIZED				
13. SUPPLEMENTARY NOTES *The Aerospace Corporation, El Segundo, CA 90245-4691, under contract to the Volpe National Transportation Systems Center -- Contract No. DTRT57-05-D-30103, Task 19 Aerospace Corporation Report No. ATR-2009(5427)-1				

14. ABSTRACT

The principles and operational characteristics of balloon and radar-based techniques for measuring upper air winds in support of launches and recoveries are presented. Though either a balloon or radar system could serve as a standalone system, the safest system would be a remote measurement system (radar or lidar) in combination with a balloon system. This would combine the accuracy, precision and reliability of a balloon system with the timeliness and localized sampling of a radar or lidar. Although numerical weather prediction (NWP) as a standalone system seems problematic, it can be employed to provide situational awareness, providing a good indication of whether conditions present at the time will or will not persist. It would also provide an understanding of the causes of changes in the weather that are being experienced and how long unsettled conditions might persist.

15. SUBJECT TERMS
Commercial Space Transportation, Regulation, Reusable Launch Vehicles, Expendable Launch Vehicles, Wind Prediction and Measurement

16. SECURITY CLASSIFICATION OF:			**17. LIMITATION OF ABSTRACT**	**18. NUMBER OF PAGES**	**19A. NAME OF RESPONSIBLE PERSON** Ruth A. Hunter
A. REPORT U	**B. ABSTRACT** U	**C. THIS PAGE** U	UU	87	
					19B. TELEPHONE NUMBER (INCLUDE AREA CODE) (617) 494-2667

High-Altitude Wind Prediction and Measurement Technology Assessment

30 June 2009

Richard L. Walterscheid
Space Sciences Department
Space Science Applications Laboratory

Prepared for:

Volpe National Transportation Systems Center
U.S. Department of Transportation
Cambridge, Massachusetts

Contract No.: DTRT57-05-D-30103, Task 19

Authorized by: Space Systems Group

AEROSPACE
Assuring Space Mission Success

High-Altitude Wind Prediction and Measurement Technology Assessment

Approved by:
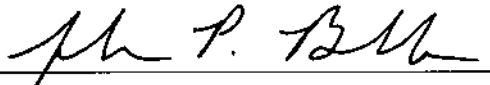
John P. Brekke, Systems Director
Civil/Commercial Launch New Business
Space Launch Projects
Launch Systems Division
Space Launch Operations
Space Systems Group
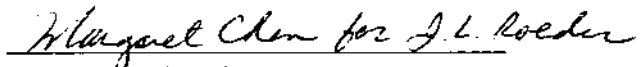
James L. Roeder, Director
Space Sciences Department
Space Science Applications Laboratory
Physical Sciences Laboratories
Engineering and Technology Group

SJ-0020(2, 5662, 91, DJ)

Abstract

The principles and operational characteristics of balloon and radar-based techniques for measuring upper air winds in support of launches and recoveries are presented.

The precise system performance (accuracy, precision, reliability) required to support reusable launch vehicle (RLV) flights is not known. Since balloon systems support launches of large expendable launch vehicles (ELVs) and the Space Shuttle, it seems likely that they would be sufficiently accurate and dependable to support RLV launches. Since performance of large powerful radars such as the Eastern Range (ER) and Western Range (WR) 50 MHz radars approaches that of balloons, these most likely would also be adequate. Less certain is the adequacy of less capable radars, present Light Detection and Ranging (lidar) systems and numerical weather prediction (NWP).

It takes an hour or more for balloons to reach their limiting altitude, and in that time they can drift distances of 100 km or more. This occurs when winds are strongest and most likely to be an operational factor. The ascent time for balloons limits the timeliness of the data. Doppler radar profilers offer the important advantage that the measured winds are overhead and that a complete profile can be obtained for some systems in 15 minutes or less. Lidars have advantages similar to radar profilers, but lack an all-weather capability. However, launches could be subject to lightning flight constraints, which limit launches in many cases where there is significant cloudiness. Lidars offer the advantage of mobility. Future lidars are expected to provide a good solution for locations that are not limited by layered clouds when lightning constraints allow flight. Numerical weather prediction models are less accurate than measurements but can be used to anticipate changes.

The safest system would be a remote measurement system (radar or lidar) in combination with a balloon system. This would offer the accuracy, precision, and reliability of the balloon system with the timeliness and localized sampling of a radar or lidar. Although numerical weather prediction as a standalone system seems problematic, it can be employed to provide situational awareness, providing a good indication of whether conditions present at the time will or will not persist. It would also provide an understanding of the causes of changes in the weather that are being experienced and how long unsettled conditions might persist.

Acknowledgments

Executive Summary

1.   Introduction

The Aerospace Corporation was tasked by the Volpe National Transportation Systems Center to assess existing technologies available for determining wind conditions at high-altitude in support of Reusable Launch Vehicle (RLV) launches in remote locations that are licensed by the FAA Office of Commercial Space Transportation (FAA/AST). This document presents an overview of the technologies for gathering wind data and atmospheric models for predicting winds. Aerospace is pleased to submit this final report that addresses accuracy, sensitivity to wind conditions, and makes recommendations based on accuracy and feasibility. It also presents an assessment of possible upgrades to extend the vertical coverage for Doppler Radar Wind Profilers (DRWPs)

Within the Commercial Space Launch Amendments Act of 2004, Congress authorized the Federal Aviation Administration (FAA) to promulgate regulations in the areas of experimental permits and human spaceflight (crew and passenger) requirements. Legislation was written to allow humans to travel into space for the first time on commercial launch vehicles and to ensure that the passengers and crew involved in commercial space are informed of all risks inherent to space travel, including those associated with the launch vehicle. Commercial launch sites have limited equipment and real-time data to support real-time launch decision making. In particular, there is a relative paucity of wind data from 50,000 ft (the altitude reliably attained by high resolution balloon measurements) and 100,000 ft (the altitude attained by low resolution systems and high performance radars). Significantly higher altitudes would require some development. The altitude limitations are mitigated by the fact that by 100,000 ft ($\sim$ 30 km) air density is reduced from sea values by a factor of $\sim$ 100. The aerodynamic drag on vehicles and debris is similarly reduced. This study evaluates technology to detect winds at these altitudes. Accurate wind data at these altitudes is very important for suborbital RLVs because of the lack of time to adjust the trajectory once the main engine cut-off has occurred. In addition it is important to characterize the tendency of winds to move debris laterally as it falls. The dispersion of debris by the winds increases the risk on the ground and in the air, when risk to aircraft is considered. This study presents the results of a literature survey of possible remote sensing technologies and the sensitivity of proposed systems to high altitude wind conditions.

2.   Data Quality

There are tradeoffs between accuracy, precision, and resolution. To obtain high precision one must sample the signal over a greater atmospheric layer thickness or time. This can degrade spatial or temporal resolution and decrease accuracy by smearing out thin features. The optimal combination of resolution, accuracy, and precision is determined by the flight system and flight constraints.

3.   Measurement Systems

Three systems for measuring winds are considered in this report and are discussed below.

3.1   Doppler Radar Wind Profilers

Doppler radar wind profilers (DRWPs) are radars that use the wind induced Doppler shift of the returned radar signal to infer air motion along radar beams [Birkemeier et al., 1968; van de Kamp, 1988; Ecklund et al., 1987]. The Doppler shift of the back-scattered energy is determined,

and used to calculate the velocity of the air toward or away from the radar as a function of line-of-sight range. The source of the backscattered energy is small-scale turbulent fluctuations that induce irregularities in the refractive index of the atmosphere. The fundamental assumption is that these irregularities move with the wind [Hollerman, 2003]. Profilers work best for regions of strong turbulence and high humidity [Brode, 2000].The motion along radar beams in different directions is projected geometrically to give the winds in the east-west and north-south directions [Schumann et al., 1999; Beran and Wilfong, 1998].

3.1.1   System Performance and Characteristics

The strength of the returned radar signal is proportional to the product of the transmitted power and the antenna aperture (power aperture product). The performance improves with higher power aperture product. The line of sight resolution of the system is a function of the pulse length and the signal-to-noise ratio [Beran and Wilfong, 1998; U.S. Environmental Protection Agency (EPA), 2000].

Antennae for DRWPs are phased arrays with a number of radiating elements. Beams are formed and steered with the use of constructive and destructive interference by shifting the phase of the signal emitted from each radiating element relative to the others. Popular choices of radar frequency are 50 MHz, 449 MHz and 915 MHz [Brode, 2000]. The altitude range of the 50 MHz systems is greatest (2-20 km), the 400 MHz system is intermediate (0.2 – 14 km) and the 1000 MHz system is least (0.1 – 5 km).

3.1.2   Data Reduction and Quality Control

The central problem of successful data reduction is to identify the Doppler shift from the Doppler spectrum that originates from the random motion of turbulent eddies. One must also account for spurious signals from fliers (e.g., planes, birds, and insects), radio-frequency interference (RFI), precipitation, ground (ground clutter) and. signals entering radar sidelobes (secondary beams formed by the antenna).

The typical signal-processing scheme for the National Oceanic and Atmospheric Administration (NOAA) Doppler radar wind profilers and many others involves consensus averaging: averaging of a subset of data that are within some error tolerance of a model value [Fischler and Bowles, 1981]. To produce high-quality wind profiles in minimal time and give better unattended results, the National Aeronautics and Space Administration, Kennedy Space Center (NASA/KSC) replaced consensus signal processing with one that uses a median filter to remove spurious echoes and constrains the search by a first guess [Wilfong et al. 1993b; Schumann et al. 1999].

3.1.3   Operational Systems

NASA/KSC 50 MHz Doppler Radar Wind Profiler: The Kennedy Space Center (KSC) and Western Range (WR) each have a profiler operating at 49.25 MHz. In nominal operation the vertical range is from about 2 km to about 18.5 km. The signal processing technique allows the extraction of complete wind profiles in 3 minutes.

NOAA 449 MHz Doppler Radar Wind Profiler: The 449 MHz system is an integral part of the NOAA network. It produces consensus averaged wind products each hour. A six minute cycle is complete by spending 1 minute in each beam in each mode (a high and low resolution mode in each of three beams) [Beran and Wilfong, 1998, Brode, 2000; WRIH, 2007; ERIH, 2007].

<u>Eastern and Western Ranges 915 MHz Doppler Radar Wind Profilers</u>: This network is designed to provide three-dimensional wind direction and speed estimates in the boundary layer from 120 m to 4 km above ground level (AGL) [Beran and Wilfong, 1998; Heckman, 1996]. Consensus data reduction is used.

3.1.4 Limitations

Signal processing is the largest problem limiting the application of wind profiler technology. Conditions may develop in the atmosphere s where there is insufficient refractive index gradients or turbulence to produce a significant reflection [Beran and Wilfong, 1998; Schumann et al., 1999].The absence of scatterers leads to gaps in the radial velocity data [Hollerman, 2003]. Though nearly all-weather, DRWPs are sensitive to precipitation to some degree. [Schumann et al., 1999].

3.2 Doppler Lidar

The basic principle of Doppler Light Detection and Ranging (lidar) is the same as for Doppler radar. The underlying principle is to measure the wind radial velocity by tracking the backscatter signal from molecules and aerosol particles (suspended particulate matter) [Rocadenbosch, 2003].

As for radar profilers, the primary design factor of a lidar system is the product of the average laser power times the aperture [Wandinger, 2005]. The backscatter coefficient for aerosols and molecules and is the primary atmospheric parameter that determines the strength of the lidar signal. Aerosol scattering is highly variable and systems that depend on aerosol scattering are sensitive to this variability. In the troposphere and lower stratosphere the aerosol scattering dominates, while at higher altitudes the molecular scattering dominates [Werner, 2005].

Aerosol detection (Coherent Detection) requires phase coherence across the field of view of the receiving optics and requires diffraction limited optics and limits the maximum size of the receiving telescope [Rocadenbosch, 2003]. The molecular (Direct Detection) method does not require diffraction limited optics or phase coherence and therefore imposes no limitation on telescope size. However, accuracy is reduced because the width of the Doppler peak for molecular scatter is much broader than the width of for aerosol scatter and it is harder to assess where the spectral peak is located.

3.2.1 Direct Detection vs. Coherent Detection Tradeoffs

Coherent heterodyne detection differs from Direct Detection in the need for a pulsed ultra stable high power laser; a second narrow-frequency laser; a fast detector; averaging over several shots to average out speckle, and the presence of aerosols [Werner, 2005]. We conclude that for reliable support of RLV operations to altitudes of 25 km when aerosol concentrations are low Direct Detection methods are required.

3.2.2 Current Systems

Wavelengths depend on the application and extend from ~ 250 nm to 11 µm. To meet eye safety requirements UV wavelengths such as those near 0.35 µm are used [Werner, 2005; Gentry et al., 2000, McGill , and Spinhirne, 1998]. .Light pulses with lengths of a few to several hundred nanoseconds (~1 to ~ 100 m) are generated [Wandinger, 2005]. Typical laser energy per pulse are 70 mJ with a telescope-scanner aperture 0.45 m [Gentry et al., 2005].

Some systems that measure winds at lower altitude, within the boundary layer, are commercially available. See for example http://www.tpub.com/content/nasa2000/NASA-2000-cr210288/NASA-2000-cr2102880097.htm. At this writing there does not appear to be any commercially available systems that can measure winds in clear air.

Lidar systems for launch support are under development. An example is the direct detection Goddard Lidar Observatory for Winds (GLOW) instrument. Compared with wind profile data from a collocated radiosonde differences indicate that the GLOW RMS accuracy below about 8 km varies between ~1 and a few m/s, with accuracy decreasing at higher altitudes. When aerosol concentrations are high the coherent systems are highly accurate, ~1 m/s or better [Ishii et al., 2005], and, in principle, a direct detection and coherent system could operate at the same site to offer the advantages of both. Hybrid systems with both direct and coherent detection have been proposed [Emmitt, 2004].

3.3 Balloon Systems

To a good approximation, rising balloons drift with the horizontal flow in which they are imbedded. Presently, balloons are the primary means of deducing winds for launch support. The primary balloon systems used to support launches on the national ranges today are the radar-tracked Jimsphere and Global Positioning System (GPS) tracked Automated Meteorological Profiling System (AMPS). Balloon- systems offer highly accurate high-resolution measurements.

3.3.1 Radar-tracked Jimsphere

The radar-tracked Jimsphere has been the benchmark for high resolution wind measurements in support of launches for the last 35 years. The wind computation begins with 100-ft layers. The processing program attempts to maintain 1 m s^{-1} precision in each wind component by increasing the averaging layer up to 400 ft [Wilfong et al., 1997].

3.3.2 Automated Meteorological Profiling System (AMPS)

The AMPS system uses Differential GPS to obtain profiles of wind velocities. The AMPS provides accurate, high-resolution profiles of wind up to 30 km [ERIH, 2007]. AMPS flight elements are a High Resolution Flight Element (HRFE) and a Low Resolution Flight Element (LRFE). The HRFE consists of a GPS radiosonde attached to a Jimsphere balloon and is used to produce high-resolution measurement of wind up to ~ 17 km. The LRFE consists of a standard helium filled latex meteorological balloon, and produces winds from the surface to near 35 km [ERIH, 2007; Leahy, 2004]. At the Eastern Range AMPS balloons run several hundred dollars each counting the balloon, sonde, helium and labor [Dr Merceret, Applied Meteorological Unit, KSC].

4. Extension of DRWP Altitude Coverage

Extension of altitude coverage means increasing the Signal-to-Noise Ratio (SNR). There are four ways to improve the SNR: Increase the aperture, the power, the vertical averaging interval, and the integration time between profiles. Improved signal processing would also help. Dr. Merceret [Applied Meteorological Unit, NASA/KSC] believes a profiler in the 40 - 60 MHz range (lower is better) could be configured to work to 150 kft (45 km) provided that it uses software at least as good as that presently used by KSC, and goes to 1-km gate spacing and integration times as much

as an hour. The power-aperture product would also have to be at least as large as the present KSC system

5. Wind Modeling

First principles dynamical models have been developed having considerable forecasting skill compared to climatological models (e.g., monthly means). The most promising are the mesoscale models with their high resolution and ability to include local influences such as topography and surface conditions.

5.1 Mesoscale Models

Mesoscale models have limited area domains that may be relocated for a given site or area. Some models have nested domains that have finer resolution for the inner domains than for the outer. Vertical resolution may be variable as well, with finer resolution near the ground than in the upper levels [Pielke and Pearce, 1994].

5.1.1 Mesoscale Model 5 (MM5)

The Mesoscale Model Version 5 (MM5) was co-developed by Pennsylvania State University and the National Center for Atmospheric research [Grell et al., 1995; Anthes and Warner, 1978; Anthes et al. 1987]. The MM5 has been continuously improved by users at universities and government laboratories [Anthes, 1972, 1977; Anthes and Warner, 1978; Anthes et al., 1987]

Verification statistics for various sites in the southwestern United States covering the area where present commercial launch sites are located was provided by Mr. Robert Craig [Air Force Weather Agency, Offutt AFB, NB]. The model data are compared to from standard meteorological soundings (rawinsondes). The data cover the approximate altitude range from 9.7 to 21 km. Generally, the bias is less than ~ 1 m/s for altitudes at and below 16 km.. The variation in accuracy between locations is not great indicating the model accuracy at is not overly sensitive to local conditions.

5.1.2 Weather and Research Forecast (WRF) Model

The *Weather and Research Forecast* (WRF) model is a new generation model developed through a collaborative partnership involving government civil and military centers and universities. It incorporates advanced numerics and data assimilation techniques, a multiple relocatable nesting capability, and an improved physics package, particularly for treatment of convection and precipitation. It is intended for a wide range of applications, from idealized research to operational forecasting [Michalakes et al., 2001]. The WRF model forecast domain can be relocated for any location. The altitude range is configurable. The only limitation is the altitude coverage of the data used to initialize the model (up to ~ 30 km, in practice).

5.2 Comparison Between MM5 and WRF Models

At most altitudes accuracy and precision for the two models are similar. Biases are generally less in magnitude than 1 m/s. Root-mean-square errors are a few meters per second. Despite the near parity in present accuracy, the WRF model is in its formative stages and should improve. The MM5 is no longer supported by annual user meeting at the National Center for Atmospheric Research (NCAR) and the pace of future improvements will most likely be limited.

6. Wind Technology Comparisons

The nominal performance of the three primary systems used to support launch activities is shown in Table 1. The advantages and disadvantages of each system are also summarized.

Table 1. Summary of System Capabilities

	Type	Vertical Range (km)	Vertical Resolution (m)	Bias (m/s)	Precision (m/s)	Advantages	Disadvantages
Balloon (1,2,3)	AMPS High Res	17	160	≤ 0.7	0.6	Highest accuracy and vertical resolution. All weather.	May take ~ hour or more to retrieve entire profile. Balloon may drift 10s of kilometers during ascent. For radar-tracked balloons drop out and sideband acquisition may occur
	AMPS Low Res	33	350	0.7	1.0		
	Jimsphere	17	100-300	≤ 0.7	0.5 + 1% of layer wind speed		
Doppler Radar (1,4,5, 6,7)	50 MHz	20	500	0.1	1.5	Good accuracy and resolution. All weather. Good temporal resolution. Retrievals for wind overhead	Not mobile. Subject to ground clutter, sideband ambiguities and spurious reflections. Dropout due to low signal (weak turbulence) may occur.
	UHF	5 (915 MHz) - 14 (404 MHz)	---	<1.7	1.7		
Lidar (8)	GLOW	25	200	---	3 up to ~ 12 km altitude	Good accuracy and resolution. Good temporal resolution. Retrievals for wind overhead. Easier to locate near launch site.	Not all weather. Technology not as mature and performance is not as well characterized. Requires periodic calibration.
Mesoscale Models	MM5 (AFWA)	20 (50 hPa)	Config-urable	1	5	Inexpensive. Can be run from one location for arbitrary site.	Subject to model biases for different locations (forecast mode). Less accurate than collocated observations.
	WRF (AFWA)	32 (10 hPa)	Config-urable	1	5		

(1) ERIH, 2007; (2) Leahy, 2004; (3) Wilfong et al., 1997; (4) Printer et al., 2006; (5) Merceret, 1999; (6) Frisch et al., 1986; (7) Strauch et al., 1987; (8) Gentry et al., 2000.

7. Recommendations

The precise system performance (accuracy, precision, reliability) required to support RLV flights is not known. Clearly, since balloon systems support launches of large expendable vehicles (that are highly wind sensitive) and the Space Shuttle they are accurate and dependable enough to support RLV launches. Since the performance of the large powerful radars such as the ER and WR 50 MHz radars approach that of balloons these most likely would also be adequate. Less certain is the adequacy of less capable radars, present lidars and numerical weather prediction.

It takes an hour or more for balloons to reach their limiting altitude, and in that time they can drift distances of 100 km or more. This occurs when winds are most likely to be an operational factor. The ascent time for balloons limits the timeliness of the data, unless more than one balloon at a time is tracked. Doppler radar profilers offer the important advantage that the measured winds are overhead and that a complete profile in 15 minutes, or less, is possible. Lidars have advantages similar to radar profilers, but lack an all-weather capability. However, launches subject to lightning flight constraints can be limited in many cases where there is significant cloudiness [Krider et al, 2006]. Lidars offer the advantage of mobility. When operational systems are developed, lidars could provide a good solution for locations that are not too limited by layered clouds when lightning constraints allow flight. While numerical weather prediction models are less accurate than measurements, they cannot be ruled out as standalone systems in the absence of wind accuracy requirements.

The safest system would be a remote measurement system (radar or lidar) in combination with a balloon system. This would offer the accuracy, precision, and reliability of the balloon system with the timeliness and localized sampling of a radar or lidar. Although NWP as a standalone system may not be feasible at this time, it can be employed to provide situational awareness and to anticipate changes in wind conditions.

Table 2 summarizes the vertical range of the systems considered in this report in both metric and English units.

Table 2. Summary of Approximate Vertical Coverage for Various Systems

Method	Peak Altitude Capability (km)	Peak Altitude Capability (ft)
Doppler radar	20	65,000
Doppler lidar	25	82,000
Jimsphere	17	56,000
AMPS (High res)	17	56,000
AMPS (Low res)	33	108,000
WRF model	32*	105,000*

*Configurable: The basic limitation is the altitude coverage of the data
used to initialize the models, up to ~ 32 km (105,000 ft) in practice.

Contents

Figures

Tables

1. Introduction

Recent events within the commercial space sector (Ansari X-Prize, Commercial Space Launch Amendments Act (CSLAA) of 2004, and X Prize Cup), are helping to spawn an emerging space tourism industry. Within the CSLAA, Congress authorized the FAA to promulgate regulations in the areas of experimental permits and human spaceflight (crew and passenger) requirements. The experimental permit legislation was enacted in an effort to lessen the regulatory burden on emerging space companies and to allow them to conduct research and development tests before applying for a launch license. Legislation for human spaceflight was written to allow humans to travel into space for the first time on commercial (non-Government) launch vehicles and to ensure that the passengers and crew involved in commercial space are informed of all risks inherent to space travel, including those associated with the launch vehicle.

The direct result of this legislation has led to an increase in commercial reusable launch vehicles operating out of commercial (non-Government) launch sites. Unlike Government launch sites (which have dedicated meteorological staffs and equipment), commercial launch sites have very limited equipment and real-time data to support real-time decision making for launch.

In particular, there is a relative paucity of wind data from 50,000 ft (the altitude reliably attained by high resolution balloon measurements) and 100,000 ft (the altitude attained by low resolution systems and high performance radars). Significantly higher altitudes would require some development. The altitude limitations are mitigated by the fact that by 100,000 ft (~ 30 km) air density is reduced from sea values by a factor of ~ 100. The aerodynamic drag on vehicles and debris is similarly reduced. This study compares and evaluates remote sensing technology to detect winds at these altitudes. Accurate wind data at these altitudes is very important for suborbital RLVs because of the lack of time to adjust the trajectory once the main engine cut-off has occurred. In addition it is important to characterize the tendency of winds to move debris laterally as it falls. The dispersion of debris by the winds increases the risk on the ground and in the air, when risk to aircraft is considered. This study will conduct a literature survey of possible remote sensing technologies and the sensitivity of proposed systems to high altitude wind conditions.

2. Measures of Data Quality

The primary measures of quality for wind measurements are accuracy, precision and resolution.

2.1 Accuracy

The accuracy of a measurement reflects how well it measures the truth. If the truth is known then the accuracy is defined as the mean difference between the truth and the measured wind components. The standard components of the wind are the eastward and northward components, denoted the u and v, respectively. The accuracy in mathematical terms is

$$\bar{u} = \frac{1}{N}\sum_{i=1}^{N}\left(u_i - \hat{u}_i\right) \qquad (2\text{-}1)$$

$$\bar{v} = \frac{1}{N}\sum_{i=1}^{N}\left(v_i - \hat{v}_i\right) \qquad (2\text{-}2)$$

where the careted quantities denote truth, N is the number of measurements and the subscript i denotes an individual instance. In general, the truth is not known and instead measurements taken to be a good standard are used.

2.2 Precision

Precision is a measure of the repeatability of the measurement. Mathematically,

$$V(u) = \frac{1}{N}\sum_{i=1}^{N}\left(u'_i - \hat{u}'_i\right)^2 \qquad (2\text{-}3)$$

$$V(v) = \frac{1}{N}\sum_{i=1}^{N}\left(v'_i - \hat{v}'_i\right)^2 \qquad (2\text{-}4)$$

where V is the variance and $u' = u - \bar{u}$. Precision is the square root of the variance.

2.3 Resolution

Resolution refers to the ability of a measurement to resolve a feature (shear, gust, jet, etc.) in the atmosphere. In spatial terms resolution is given by the region sampled to make a single determination of wind. In spectral terms the smallest wavelength that can be resolved in principle is the Nyquist (twice the sampling interval). However, in practice the smallest feature that can be resolved is where the signal spectrum falls below the noise spectrum [Merceret, 1999].

2.4 Tradeoffs

There are tradeoffs between accuracy, precision, and resolution. To obtain high precision one must average measurement collected over intervals of time or altitude. This can degrade spatial or temporal resolution, or increase the bias (decrease accuracy). The decrease in accuracy comes

from the fact that excessive averaging can smear out features such as thin jets. The optimal combination of resolution, accuracy and precision is determined by the application of the data.

3.   Measurement Systems

In this chapter the principles of operation for the systems used for making wind measurements to support launches are discussed.

3.1   Doppler Radar Wind Profilers (DRWPs)

Doppler profilers are radars that use the Doppler shift of the returned radar signal to infer air motion along radar beams [Birkemeier et al., 1968; van de Kamp, 1988; Ecklund et al., 1987]. The radar transmits pulses along each of the antenna's pointing directions. The duration of a pulse determines its length and the volume of air illuminated. Small amounts of the transmitted energy are scattered back toward the radar. Delays of fixed intervals are built into the data processing system so that the radar receives scattered energy from discrete altitudes, referred to as range gates. The Doppler frequency shift of the backscattered energy is determined, and then used to calculate the velocity of the air toward or away from the radar along each beam as a function of altitude. The source of the backscattered energy is small-scale turbulent fluctuations that induce irregularities in the refractive index of the atmosphere at radar frequencies. The fundamental assumption is that these irregularities move with the wind [Hollerman, 2003]. The radar is most sensitive to scattering by turbulent eddies in density and water vapor whose spatial scale is ½ the wavelength of the radar (the Bragg Scale) [Brode, 2000].

The fundamental process upon which Doppler systems are based is the frequency shift of a signal seen by an observer when the source of the signal is approaching or receding. For electromagnetic signals

$$f_d = f\left(1 + 2\frac{v}{c}\right) \tag{3-1}$$

where f_d is the Doppler shifted frequency, f is the frequency of the source, v is the radial velocity relative to the observer (positive for motion toward the observer and negative for motion away), and c is the speed of light. Higher order terms have been ignored. If f_d, and f are known then v can be calculated from (1) [Hollerman, 2003].

3.1.1   Atmospheric Turbulence as Markers of Wind

As mentioned, the returned radar signal results from scattering from turbulent structures in the refractive index of air. Profilers work best for regions of strong turbulence and high humidity and least well for regions of smooth dry air [Brode, 2000].

The greater the altitude is, the weaker the return. Two factors are responsible for the diminishment of the returned signal with altitude. First, beam spreading and scattering into all directions results in the returned power decreasing approximately proportionate to the inverse fourth power of the altitude. Second, the back-scattered power for a density fluctuation of fixed percentage with respect to the background air density is proportional to the background density. Air density decreases approximately exponentially with altitude by a factor of about 10 for every 16 km. This means that with every 16 km increase in altitude for the same percentage fluctuation in density, the ambient density would return power reduced roughly a factor of 10.

In applying the Doppler shift (1) to obtain wind profiles, it is assumed that the scatterers are markers of the air motion. However, turbulence structures (eddies) will in general have motion relative to the bulk flow [Lumley and Panovsky, 1964]. The velocities of eddies relative to the bulk flow should be close to zero on average. This means that a suitable measure of the central tendency of the Doppler shifts should give a good measure of the bulk motion.

The Doppler shift gives the velocity in the radial direction (that is, along the line-of-sight). Since the wind vector has three components, a minimum of three viewing directions is required to fully represent the wind. However, under most conditions the vertical wind component is small and the wind may be regarded as horizontal (two dimensional). It is then adequate to use two off-vertical beams [Schumann et al., 1999].

To derive winds one must assume that the wind is the same at each location during the time it takes to make a single wind determination. However, beams illuminate different spots in the sky at a given altitude and may illuminate them at different times. The validity of the assumptions of uniformity and stationarity depends on wind conditions, the separation between beams, and the time interval over which the measurement is made. Uniformity and stationarity are favored by small beam separations and a short cycle time between beams. On the other hand, one wants the beam separation to be large enough so that the horizontal winds to project well on the line of sight. One also wants the time separation to be large enough to minimize the effects of short-lived eddies. Off-vertical angles on the order of 15° to 20° are typical [Beran and Wilfong, 1998].

3.1.2   The Doppler Spectrum

The random motions of eddies and the effects of shear within the illuminated volume broaden the Doppler spectrum. The width of the Doppler spectrum depends on the distribution of the eddy velocities along the line of sight [Beran and Wilfong, 1998].

3.1.3   System Sensitivity

The scattered power P_r received is given by the radar equation

$$P_r = \frac{P_t G_t A_r \sigma F^4}{(4\pi)^2 R^4} \qquad\qquad (3\text{-}2)$$

where P_t is transmitter power, G_t is gain of the transmitting antenna, A_r is effective aperture (area) of the receiving antenna, σ is the radar cross section or scattering coefficient of the target, F is pattern propagation factor, R is distance from the transmitter to the target [Byron, 1992; http://en.wikipedia.org/wiki/Radar, 2009]. The pattern propagation factor accounts for factors such as multipath. The power of the returned signal is proportional to the product of the transmitted power and the antenna aperture (power aperture product).

The performance of any wind profiler is limited by its sensitivity, which improves with higher power aperture product. Data quality is improved by increasing the number of beams. The line of sight resolution of the system is a function of the pulse length and the signal-to-noise ratio [Beran and Wilfong, 1998; EPA, 2000].

3.1.4 Antenna Configuration

Antennae for DRWPs are phased arrays consisting of a number of radiating elements, each with a phase shifter. Beams are formed by means of constructive and destructive interference by shifting the phase of the signal emitted from each radiating element. The beam is steered by changing the phase shift between elements. The dwell time for each beam is typically a few tens of seconds [Schumann et al., 1999]. Figure 3-1 shows a schematic view of the beams formed by a phased array antenna.
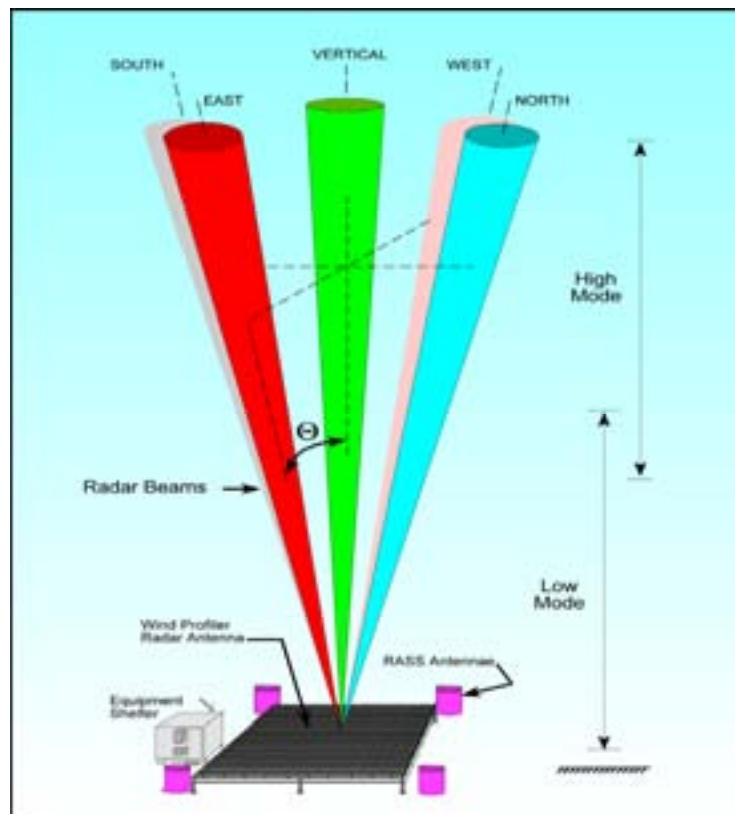
Figure 3-1. Typical Wind Profiler Beam Configuration Consisting of Three to Five Beams. One is vertical, and two or four are tilted near 15 degrees from the zenith in orthogonal directions [Fig. 2-1, Beran and Wilfong, 1998]. Image reprinted courtesy of the Office of the Federal Coordinator for Meteorology.

If the assumption of local horizontal uniformity is met and the return signal is strong enough, then only one cycle of the antenna beam pointing position is needed to measure the wind. However, time-height profiles of wind data show that local horizontal uniformity is rarely, if ever, satisfied [Beran and Wilfong, 1998]. The largest single advantage a 4 or 5 beam system offers is the capability to check the basic assumptions of horizontal homogeneity and stationarity; and therefore, produce more reliable products [Beran and Wilfong, 1998].

3.1.5 Radar Frequencies

Operating characteristics of three common types of radar wind profilers are given in Table 3-1. The categories are: very high frequency (VHF) profilers that operate at frequencies near 50 MHz; ultra-high frequency (UHF) tropospheric profilers that operate at frequencies near 400 MHz; and

UHF lower tropospheric profilers that operate at frequencies near 1000 MHz. Popular choices
are 50 MHz, 449 MHz, and 915 MHz Brode, 2000].

Table 3-1. Characteristics of Radar Wind Profilers [Table 9-13, Brode, 2000]

Frequency Class	Antenna Size (m^2)	Peak Power (kw)	Range (km)	Reso-lution (m)	Alias and Prototypes
50 MHZ	10,000	250	2-20	150-1000	Alias: VHF radar wind profiler Prototype: 50 MHZ (600cm) profiler used in the Colorado Wind Profiler Network in 1983
400 MHZ	120	40	0.2-14	250	Alias: UFH (tropospheric) radar wind profiler Prototypes: 404 MHZ (74cm) profiler developed for the Wind Profiler Demonstration Network (WPDN) in 1988. 449MHZ (67cm) profiler operates at the approved frequency for UHF profilers and will eventually replace the 404 MHZ units 482 MHZ (62cm) profiler used by the German Weather Service
1000 MHZ	3-6	0.5	0.1-5	60-100	Alias: UHF lower-tropospheric radar wind profiler Boundary layer radar wind profiler Lower-atmospheric radar wind profiler Prototypes: 915 MHZ (33cm) profiler used in the Colorado Wind Profiler Network in 1983 1290 MHZ (23 cm) boundary layer profiler used by the German Weather Service

Radars with different frequencies have different Bragg scales (the scales where scattered radiation
constructively interferes, here the smallest such scale). The higher the frequency the smaller is
the eddy scale to which the radar is most sensitive. The 50 MHz profilers are sensitive to scales
near 3 m. A profiler operating at 449 MHz is sensitive to scales near 40 cm. Normally, the
spectrum of atmospheric turbulence has more energy at larger scales [Lumley and Panofsky,
1964]. Everything else being equal, the energy returned by a 50 MHz system should be greater
than that for a 449 MHz system.

3.1.6   Pulse Length and Resolution

Profilers are capable of generating more than one pulse length. The 50-MHz Radar Wind
Profiler/RASS (RWP50), for example, is capable of pulse lengths of 250, 500, 750, 1000 m
[Coulter, 2004]. Shorter pulse lengths (high resolution mode) may be used for low altitudes and
longer pulse lengths (low resolution mode) for high altitudes. There is a tradeoff between
resolution and power returned since a greater volume is illuminated, the longer the pulse, the
lower the resolution. Delays of fixed intervals are built into the data processing system so that the
radar receives scattered energy from discrete altitudes, referred to as range gates [Hollerman,
2003].

3.1.7 Radar Power

Table 3-1 indicates that 50 MHz systems have power typically ~ 250 kW while 400 MHz systems have ~ 40 kW. The power of 1000 MHz systems is much less, being ~ 0.4 kW [Brode, 2000]. Commensurate with the power, the vertical range of the 50 MHz systems is greatest (2-20 km), the 400 MHz system is intermediate (0.2 – 14 km), and the 1000 MHz system is least (0.1 – 5 km). Other factors, such as aperture and Bragg scale, also have a role in determining range.

3.1.8 Data Reduction and Quality Control

Signal processing is the largest problem limiting the application of wind profiler technology. The central problem of successful data reduction is to distinguish the Doppler shift from the Doppler spectrum. One must also account for spurious signals. In this section, we briefly discuss standard DRWP signal processing. Modifications that are applied to specific systems will be discussed below.

The typical signal-processing scenario for the National Oceanic and Atmospheric Administration (NOAA) and many other Doppler radar wind profilers involves calculating a consensus average on a gate-by-gate basis. Consensus averaging selects a subset of data in a set of points that will be used to make a measurement. An initial subset comprising the minimum number of points required to perform a suitable average of the data the data is chosen. Next the points that are within an error tolerance of the average are determined. This set is called the consensus set. This process may be iterated to get a new model fit and a new consensus set. The process halts when the consensus set is deemed large enough, or when the process fails to find a minimum set. The average when the process successfully halts is the consensus average [Barth et al, 1994; Fischler and Bowles, 1981]. Consensus averaging is capable of smoothing data that contain a significant percentage of gross errors.

Winds from the national network are quality controlled at the NOAA wind profiler hub using continuity checks before they are distributed [Wuertz and Weber, 1989; Weber and Wuertz, 1991; and Weber et al., 1993]. These additional quality control measures identify suspect winds after they are computed.

The standard consensus-average technique delivered with the system was judged inadequate for launch support at the ER. NASA replaced the conventional signal processing with one that uses a median filter to remove spurious echoes from the averaged Doppler spectral data and constrains the search by a first guess [Wilfong et al. 1993b; Schumann et al. 1999].

Time height profiles of wind data show that local horizontal uniformity is rarely, if ever, satisfied. What has been demonstrated by comparisons with radiosondes is that the profiler can measure mean wind profiles when the radial velocities are averaged over a number of cycles of antenna pointing positions. The averaged radial velocities are then representative of the mean radial winds in most meteorological conditions [Beran and Wilfong, 1998]. However, with only a three-beam system, there is not enough information to make a determination regarding whether the effects of nonuniformity have been successfully removed [Beran and Wilfong, 1998]. Nominally, it takes on the order of a few minutes for a wind profiler to complete a sampling cycle.

Profiler data can have problems caused by interfering signals, even with well-designed and properly-operating systems at relatively clutter-free sites. The primary sources of interfering signals are:

<u>Ground and sea clutter</u>: Ground clutter removal is done by suppressing the Doppler signal around zero velocity, with the side-effect of biasing the winds away from zero. Jordan et al. [1997] and May and Strauch [1998] describe methods for reducing the clutter power without affecting the desired signal.

<u>Radio frequency interference (RFI)</u>: RFI is not a problem for most systems, but 449 MHz profilers can see amateur radio repeaters. In some cases it is possible to mitigate the effects of RFI, which tend to be spread over only a few kilohertz [Beran and Wilfong, 1998].

<u>Migrating songbirds</u>: Problems caused by migrating birds have received considerable attention [e.g., Wilczak et al. 1995]. Automated ways to recognize bird contamination in the wind data have been developed, for example, Merritt [1995].

<u>Atmospheric echoes in radar sidelobes</u>: Sidelobes are secondary beams that are formed by the antenna. Strong signals in antenna sidelobes can be generated by thunderstorms and strong horizontally stratified reflectivity layers. The latter usually appears in higher altitude resolution volumes. This type of interference has not been identified as a major concern in UHF profilers [Beran and Wilfong, 1998].

Current time domain and spectral processing do not effectively eliminate contamination from these sources of spurious signals. Although consensus averaging is applied to remove spurious data, contaminated measurements are still produced. Thus, before using profiler data in operational applications further quality control is necessary. For example, data from the national profiler network is assimilated and quality controlled at the hub in Boulder, Colorado before being released. In addition to data quality issues, consensus averaging also sharply reduces the frequency at which an independent wind profile can be derived [Beran and Wilfong, 1998].

The most difficult problem is when the atmospheric echo and the interfering signal have similar velocities. A number of techniques have been developed to extract estimates when the atmospheric echo is separated in velocity from the interfering signal. This is most prevalent in the lower altitude gates where ground clutter echoes are present [Beran and Wilfong, 1998].

Ultimately the signal-to-noise ratio limits the ability to extract a wind. Normally, signal-to-noise degrades with increasing line-of-sight range, limiting the maximum altitude of a wind profiler with a given power-aperture product. In addition conditions may develop in the atmosphere, such as near the jet stream where there is not sufficient density discontinuity to produce a reflection [Beran and Wilfong, 1998].

Most DRWPs function well in a broad range of frequencies. However, all DRWPs are sensitive to precipitation to some degree and the 915 MHz systems are sensitive to clouds. The higher the frequency is the greater the sensitivity. Numerous comparisons of winds measured by profilers and radiosondes [Larsen 1983] in clear air show results that are similar to radiosonde-radiosonde comparisons (on the order of 1 m/s). In precipitation, however, errors may be on the order of tens of meters per second when fall rates are not properly included, but when properly included errors are reduced to 2-4 m/s for an UHF radar. The decrease in precision comes mostly from nonuniformity from one beam to another. The effects of precipitation are discussed by Wuertz et al. (1988). Lightning generates enough of a signal at 49.25 MHz to contaminate signals when heavy thunderstorms are nearby [Schumann et al., 1999].

A Doppler radar can only determine the mean radial velocity when a scattered signal is received. The absence of scatterers leads to gaps or "no data" regions in the radial velocity data [Hollerman, 2003]. Occasionally there are regions in the atmosphere where the refractive index gradient and turbulence are so weak that the radar cannot detect a return, or the detectable return is intermittent. In such cases it may be possible to average across the gaps [Schumann et al., 1999].

Interference from strong sources of reflection in the sidelobes can be generated by thunderstorms, gradients in layer reflectivity, and objects such as birds. Improved data processing methods can eliminate most sources of sidelobe interference.

3.1.9   Operational Systems

3.1.9.1   NASA/KSC 50 MHz Doppler Radar Wind Profiler

The NASA/KSC 50 MHz wind profiler was completed 1990 as a demonstration of the ability of this technology to meet Space Shuttle launch support requirements. A nearly identical system was installed at the White Sands Missile Range at about the same time [Nastrom and Eaton, 1995] and subsequently moved to the WR. These large powerful systems are the only systems in the United States.

System hardware: The Kennedy Space Center (KSC) profiler operates at 49.25 MHz. The antenna consists of a phased array of 168 coaxial-collinear elements and has a physical aperture of 15600 m^2. Figure 3-2 shows an aerial view of the antenna for the ER system. The system operates at about a 5% duty cycle with an average power aperture of 10^8 W m^2. It is configured to generate three beams: one vertical beam and two beams inclined 15° degrees from the vertical at azimuths of 45 and 135°.

Figure 3-2. 50-MHz DRWP Antenna Field Located at KSC
[Fig. 3, Decker and Leach, 2004. Image reprinted with permission of authors.]

The system can generate either 1 or 4 µs pulses giving a vertical range resolution of 150 m (low mode) or 600 m (high mode). In nominal operation the high mode is not used. The pulse coding restricts the first useable altitude to about 2 km because of antenna ringing and system recovery time. In nominal operation the range is from about 2 km to about 18.5 km.

Data reduction: Though the consensus averaging algorithm eliminated most transient interference signals, it was found to be highly susceptible to persistent interference and often produced erroneous wind estimates [Schumann et al., 1999].Therefore the standard consensus-average technique delivered with the system was replaced with one that uses a median filter to remove spurious echoes from the averaged Doppler spectral data and constrains the search by a first guess [Wilfong et al. 1993b; Schumann et al. 1999]. The automated quality control allows the radial velocity to be replaced by the first-guess velocity when the signal to noise ratio is too low or the wind shear is too great. For launch operations, the performance of the first guess is closely monitored with provisions for an operator to reset the first guess on any gate where the winds are clearly wrong. Details may be found in Schumann et al [1997], Wilfong et al. [1993b] and Hildebrand and Sekhon [1974]. The steps that are applied on a gate-by-gate basis are shown in Table 3-2.

The median filter, first-guess technique implemented on the NASA 50 MHz system has been demonstrated to greatly improve the timeliness of the data. The technique allows the extraction of complete wind profiles in 3 minutes.

It is generally effective in eliminating spurious transient signals to remove spurious echoes from the averaged Doppler spectral data. The automated QC median filter first guess scheme implemented at KSC can catch nearly all of the sidelobes and interference signals. The small percentage of data flagged by the automated process indicates that the DRWP data produced by the algorithm are generally clean. Less than one-third of 1% of the data were flagged [Schumann et al., 1999]. During sensitive launch operations continuous interactive, manual quality control is necessary [Schumann et al., 1999; Beran and Wilfong, 1998].

Table 3-2. Steps for NASA Median Filter First-Guess Processing [Schuman et al., 1999]

Parameter	Default	Description and Effect
First-guess velocity window width	12	Constrains the search for the first velocity to six Doppler frequency bins either side of the first-guess velocity. The default is approximately equivalent to ± 1.5 m s^{-1}.
First-guess velocity	Previous radial velocity	Center of first-guess velocity window.
Integration window	20	Constrains the interval over which the signal power is calculated to 10 Doppler frequency bins either side of the maximum spectral power density. This is approximately equivalent to ± 2.5 m s^{-1}.
Cut-off percent	0.01	Percent difference between the maximum spectral power density and the spectral power density of the frequency bins included in the signal power integration. In this case the integration window limits occur when the spectral power density drops 1% from its maximum value.
Number of points in temporal median filter	3	Number of radar cycles included in the temporal filter applied to the oblique beams' spectra.
Number of points in vertical beam smooth	5	Number of points included in the running average that smooths the vertical beam's spectra.
Vertical velocity correction	Off	Determines whether or not the vertical velocity correction is applied.

Figure 3-3 shows performance data for the 50 MHz system compared to balloon data as a function of height for summer and winter and both seasons combined. The errors of the balloon data (< 1 m/s, [Wilfong, 1997]) are considered to be sufficiently small so that the differences are approximately the errors in the radar measurements. Below about 15 km the errors are < 2 m/s for the combined results, increasing to ~ 3 m/s above. Winter values are typically ~ 0.5 – 1.0 m/s greater than summer values. The differences between the beams, mainly below 8 km, reflect difference in the prevailing wind and the tendency for radar-balloon differences to be greater in stronger winds.
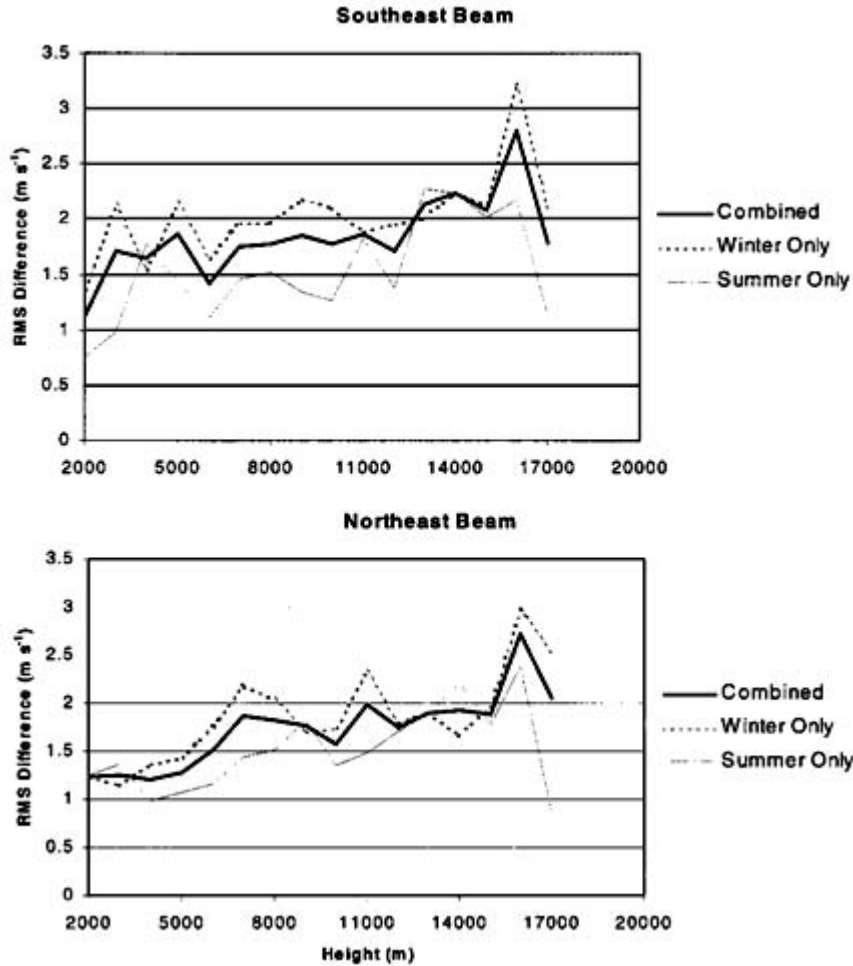
Figure 3-3. Height Distributions of RMS Differences between Jimsphere and DWRP Data for Summer and Winter and Both Seasons Combined. Balloon data are projected on the two off zenith beams of the radar for comparison [Schuman et al., 2006].

3.1.9.2   NOAA 449 MHz Doppler Radar Wind Profiler

The 449 MHz system is an integral part of the NOAA network. It produces consensus averaged wind and virtual temperature products each hour. A general description of the standard network wind profiler including system hardware and data reduction can be found in Barth et al., [1994]. A brief summary is presented here.

System hardware: The system has two modes of operation. In the low mode a 1.67 microsecond pulse gives a vertical range resolution of 320 meters; and in the high mode a 6.67 microsecond pulse gives a range resolution of 900 meters. In the low mode, the first gate is 500 meters and the highest gate is 9.25 km. In the high mode the low gate is 7.5 km and the high gate is 16.25 km. The antenna is a coaxial-collinear phased array with an effective aperture of 70 m^2. In the low mode the average transmitted power is 375 W giving a power-aperture of 2.6×10^4 W m^2. In the high mode the average power is 1500 W giving a power-aperture of about 10^5 W m^2. The antenna forms one vertical and two oblique beams with 16.3^0 off zenith pointing angles. A six minute cycle is complete by spending 1 minute in each beam in each mode. Most of the systems have a Radio Acoustic Sounding System (RASS). [Beran and Wilfong, 1998, Brode, 2000;

14

WRIH, 2007; ERIH, 2007]. (A RASS is a system where radar energy reflects from an acoustic wave front produced by the instrument). Figure 3-4 shows the distribution of the NOAA sites [http://www.profiler.noaa.gov/npn/npnSiteMap.jsp]
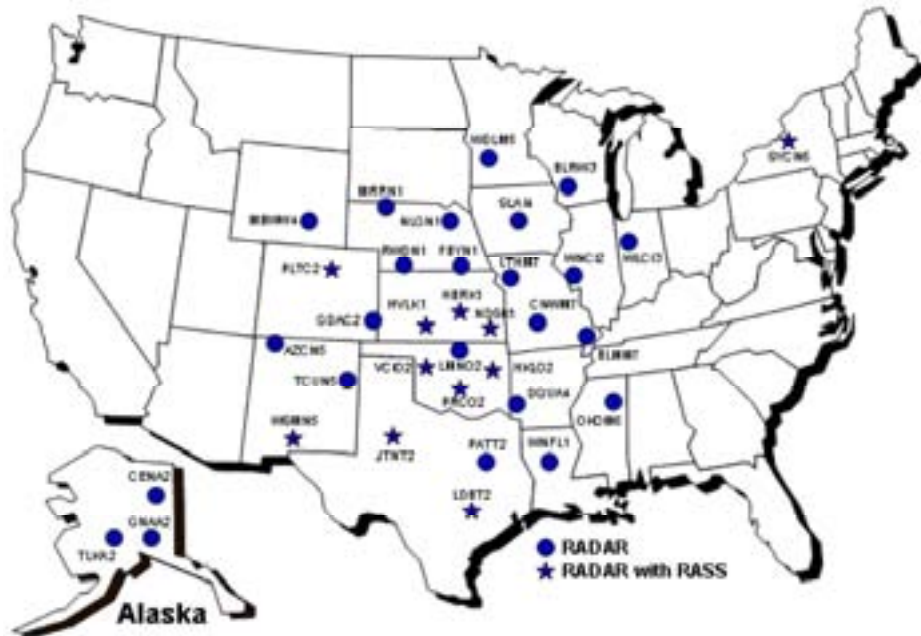
Figure 3-4. Locations of Doppler Radar Wind Profilers in the NOAA Profiler Network [http://www.profiler.noaa.gov/npn/npnSiteMap.jsp].

Data reduction: The classical consensus data reduction is used. At the end of each six minute cycle the moments are sent to the network hub in Boulder, CO where the consensus averaging wind computation and quality control are done.

3.1.9.3   Eastern and Western Range 915 MHz Doppler Radar Wind Profilers

These systems operate in the 915 MHz commercial band at low power and are designed for applications requiring only low altitude data. In 1996, the Eastern Range (ER) completed installation of a network of five 915-MHz radars with a Radio Acoustic Sounding System (RASS). This network is designed to provide three-dimensional wind direction and speed estimates in the boundary layer from 120 m to 4 km AGL [Beran and Wilfong, 1998; Heckman, 1996]. The Western Range (WR) has a suite of six 915 MHz DRWP placed at launch areas on Vandenberg AFB. Each radar operates in two different modes. One mode provides 100-m vertical resolution from 120 m AGL to 2 km. The other mode provides 200-m vertical resolution from 320 m AGL to about 3–4 km. [Beran and Wilfong, 1998; ERIH, 2007, WRIH, 2007]. The 915 MHz DRWP typically collects data on wind speed and direction from 135 m to 4,000 m. The performance of these systems varies widely depending on how the system is operated.

System hardware: The antenna consists of four panels that measure 1.23 m by 1.23 m arranged in a square array. The combination of the antenna and phase shifter allows the antenna system to point vertically and in four orthogonal directions. Of the five directions available, the ER 915

MHz radar are set to use the vertical and two orthogonal directions (north and east) [ERIH, 2007]. The WR 915 MHz radar antennas consist of a single-phased micro-strip antenna array made up of four panels.

Data reduction: The classic consensus data reduction is used. The basic system does no quality control of the meteorological products. There is an add-on product that can perform quality control of the winds using a pattern recognition technique [Weber and Wuertz, 1991; Weber et al., 1993].

3.2   Doppler Lidar

3.2.1   Principles of Operation

3.2.1.1   Introduction

Light detection and ranging (lidar) has a number of meteorological applications, including the remote sensing of winds. The basic principle of Doppler lidars is the same as for Doppler radar. The underlying principle is to measure the wind radial velocity by tracking the backscatter signal from molecules and aerosol particles [Rocadenbosch, 2003]. Doppler lidars may be pulsed or Continuous-Wave (CW). For CW systems range information is obtained by purely geometric means (focusing). Its use in practical applications is limited to altitudes below 1000 m [Werner, 2005], which removes it from further consideration for this study.

A lidar consists of a transmitter and a receiver. Short light pulses with specific spectral properties are generated by the laser. At the receiver end, a telescope collects the photons backscattered from the atmosphere. These are analyzed for the spectral characteristics and the selected radiation is directed to a detector where the optical signal is converted to an electrical signal [Wandinger, 2005].

Laser beams are highly collimated (narrow-beamed). This offers an advantage with respect to radar. First, the smaller spreading of the beam means less dilution of the signal and, second, the regions sampled are less subject to variations of the measured quantity within the field of view. Depending on the purpose of the lidar, the diameter of the primary optics varies between 0.1 m to a few meters.

Laser pulse repetition rates range from a few up to several thousand shots per second. Because the high repetition rates are not meaningful, lidar signals are normally averaged over time intervals of a few seconds to minutes. This reduces the amount of data that must be stored and decreases the variance of the measurements.

The detected signal may be written as

$$P(R) = KG(R)\beta(R)T(R) \qquad\qquad (3\text{-}3)$$

Where P is the power received from a given distance R, K summarizes the performance of the lidar system, G describes the range dependent measurement geometry, β is the backscatter coefficient and T is the transmission. The first two factors are determined by the lidar setup. The information about the atmosphere is contained in the last two factors.

The system factor can be written as

$$K = P_0 \frac{c\tau}{2} A \eta \tag{3-4}$$

Where P_0 is the average power of a single laser pulse, c is the speed of light, τ is the temporal pulse length, A is the telescope area and η is the overall system efficiency. As for radar profilers, the primary design factor of a lidar system is the product of the average laser power times the aperture [Wandinger, 2005].

The geometric factor is

$$G(R) = \frac{O(R)}{R^2} \tag{3-5}$$

where O(R) is an overlap function that accounts for incomplete imaging of the backscattered signal. The $1/R^2$ factor is primarily responsible for the large dynamic range of a lidar.

The backscatter coefficient is the primary atmospheric parameter that determines the strength of the lidar signal. In the atmosphere laser light is scattered by air molecules and aerosols. Therefore the return depends on atmospheric density and particulate concentrations. Atmospheric density decreases approximately exponentially with height. Particulates comprise a variety of scatters including sulfates, water, soot, organic compounds, dust, hydroscopic minerals and sea salt whose concentrations are highly variable in time and space [Wandinger, 2005, Rocadenbosch, 2003]. This means that systems that depend on aerosol scattering are sensitive to the variability in aerosol concentrations, and are ineffective where aerosol amounts are minimal.

The transmission T is the fraction of light that is lost on the path from the lidar to the scatterer and back. Extinction can occur as a result of absorption and scattering of light by molecules and aerosols.

In addition, the detected signal will always include a background component. In the daytime this comes primarily from direct or scattered sunlight for direct detection systems. Coherent systems are essentially free from such background noise. Detector noise is another background source. The background must be subtracted before a lidar signal can be evaluated [Wandinger, 2005].

The lidar signal is broadened by scatterer motions. For a lidar the signal is broadened by molecular motion (Rayleigh scattering) and aerosol motion (Mie scattering). These spectra appear as two superposed peaks. In the lower troposphere the Mie peak dominates, while at higher altitudes the Rayleigh peak dominates. Coherent and incoherent techniques are used in detection. Coherent detection is most commonly heterodyne detection. This involves mixing or multiplying the scattered signal with an offset frequency to produce sum and difference signals. Incoherent detection most commonly uses direct-detection to measure the spectrum of return signals or spatial-correlation techniques [Werner, 2005].

3.2.1.2   The Doppler Spectrum

The Doppler spectrum shows a tall sharp peak for aerosols and a lower broad peak for molecules (Figure 3-5)
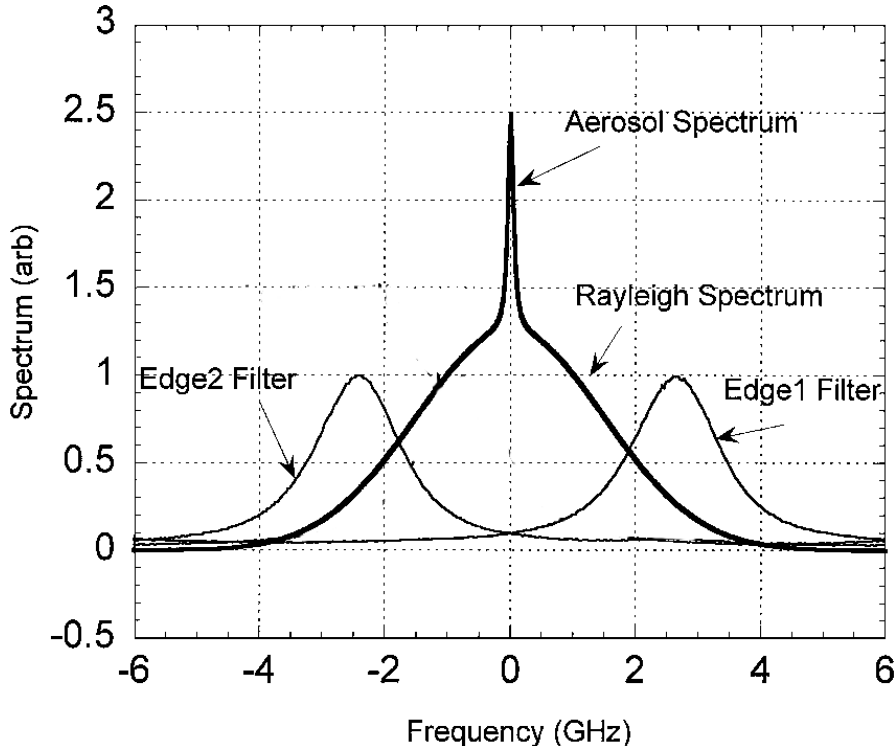
Figure 3-5. Spectra of the Atmospheric Backscattered Rayleigh and Aerosol Signals along with Two Etalon Transmission Functions. Adapted from Figure 1, Gentry et al. [2000].

3.2.1.3   Coherent Detection

Coherent heterodyne detection operates by mixing the return signal with a single-frequency local-oscillator laser prior to the optical detector. The detector operates as a photomixer and transforms the signal into an intermediate signal in the radio frequency (RF) regime. This allows the use of standard RF techniques for amplification, filtering and frequency analysis [Petheram et al., 1989]. A disadvantage of coherent heterodyne detection is that it requires phase coherence across the field of view of the receiving optics. This requires diffraction limited optics and limits the maximum size of the receiving telescope [Rocadenbosch, 2003]. Because diffraction limited optics are more difficult to make at shorter wavelengths, coherent heterodyne systems operate at longer wavelengths than direct detection systems. This means that the light scatters effectively only from the larger particles, which drop off rapidly with altitude. Coherent heterodyne systems only work when aerosols are present, but when they are present in sufficient quantity the accuracy of heterodyne system is high [Rocadenbosch, 2003].

Coherent Doppler radars operate in the 1-10 μm wavelength band. While longer wavelength minimizes atmospheric turbulence effects, significant technical advantages associated with solid-state lasers are making them increasingly more attractive compared to CO_2 lasers for coherent lidar applications.

3.2.1.4   Direct Detection

Direct detection relies on directly sensing the Doppler shift by measuring the wavelength shift of the return signal. The direct detection method does not require diffraction limited optics or phase

18

coherence and therefore imposes no limitation on telescope size. Direct detection can utilize molecular Rayleigh scattering and operate in clean air where aerosols are essentially absent [Rocadenbosch, 2003]. However, accuracy is reduced because the width of the Doppler peak for molecular scatter is much broader than the width for aerosol scatter. This makes it harder to assess where the spectral peak is located.

3.2.1.5   Direct Detection vs. Coherent Detection Trades

Coherent heterodyne detection differs from Direct Detection in the need for

- A diffraction-limited optical system and laser with near-diffraction-limited beam. A high-power laser is not required for pulsed laser with CW methods that utilize lasers which are frequency modulated. Range is determined from the intermediate frequency.

- A second frequency-stable laser called the Local Oscillator (LO)

- A fast detector in which the return and LO signals are mixed

- Time for averaging over several shots to average out speckle, and

- The presence of aerosols.

[Werner, 2005]

Where aerosol concentrations are sufficiently high, Mie scattering is much stronger for infrared and visible wavelengths than for Rayleigh scattering. Observations have confirmed the presence of a well-defined multimodal frequency distribution of aerosol backscatter values. The primary mode (the so-called "background" mode) is in the middle and upper troposphere and appears to account for 40%-50% of all tropospheric backscatter [Baker et al., 1995, Rothermel et al. 1989; Bowdle et al. 1993]. This feature is characterized by low backscatter values (i.e., 10^{-11} to 10^{-10} m^{-1} sr^{-1} at CO_2 wavelengths) and has weak spatial and temporal variability. A slightly broader secondary mode is associated with much higher backscatter in the planetary boundary layer (PBL). Together these reasonably predictable features account for more than 60% of the tropospheric backscatter. The remaining backscatter is associated with two much broader distributions from less predictable targets, namely clouds and PBL aerosols detrained into the background middle and upper troposphere ("convective mode") where they are diluted. The diluted PBL distribution lies in the gap between the PBL and the background distributions [Rothermel et al., 1989]. The cloud mode roughly overlaps the convective mode. At CO_2 laser wavelengths the cloud backscatter is about two orders of magnitude greater than the PBL mode [Menzies and Tratt 1993].

Simulations indicate that a high-resolution 355 nm system that uses the narrow aerosol peak would work well for the lower troposphere (2-3 km), but not in the upper troposphere (9-10 km) where fewer aerosols are found [Werner, 2005].

We conclude that for reliable support of RLV operations to altitudes of 50,000 ft (~ 16 km) Direct Detection methods are required. Henceforward the focus will be on Direct Detection systems.

3.2.2   System Hardware

3.2.2.1   Frequencies

Wavelengths depend on the application and extend from ~ 250 nm to 11 μm. Eye safety is often a major concern and important factor in wavelength choice. This has limited the utility of visible wavelength lasers. The eye is orders of magnitude less susceptible to laser damage in the near infrared (IR) and ultraviolet (UV) spectral regions than it is in the visible. This factor has led to an increase in the use of the third harmonic of the Nd:YAG (neodymium-doped yttrium aluminum garnet) laser at 355 nm in the UV and wavelengths near 1.5 μm in the near-IR. While CO_2 lasers were popular in the early years, high-power excimer and Nd:YAG lasers have been gaining since the 1980s. Excimer lasers produce ultraviolet radiation, while the Nd:YAG crystal emits in the infrared region at a wavelength of 1064 nm. Nowadays the doping of crystalline lattices or of gasses with active rare earth elements creates a wide range of infrared wavelengths, some of which are particularly well-suited for Doppler lidar [Wandinger, 2005]. Tunable radiation in the shortwave to long wave infrared is now produced at moderate power levels using various non-linear optical conversion techniques such as Optical Parametric Oscillators (OPOs) and difference frequency generation.

The wavelength dependence for aerosol (Mie) scattering varies between ~ λ^{-2} to λ^{+1} compared to λ^{-4} for molecular (Rayleigh) scattering. Thus the ratio of the Rayleigh signal to the aerosol background increases as the wavelength decreases. Where aerosol concentrations are low and Direct Detection is required, returns strong enough for accurate wind determination are favored by shorter wavelengths [Werner, 2005; Wandinger, 2005]. To meet eye safety requirements, UV frequencies, such as those near 0.35 μm, are used [Werner, 2005; Gentry et al., 2000, McGill, and Spinhirne, 1998].

3.2.2.2   Determination of Doppler Spectrum

For the determination of the center of the distribution, from which wind speed is obtained, two main techniques are available. One is a high-dispersion multichannel spectrometer that yields the whole spectral distribution. The other is the use of filters such as Fabry-Perot interferometers or etalons. Because the Doppler shifts are so small and the spectral peak is so broad, two identical filters (except for central frequency) are disposed symmetrically on either side of line center at the edge of the transmission curve where the filter transmission function is changing most rapidly. This is shown schematically in Figure 3-3. To avoid contributions from the central Mie peak the filter transmission functions should go to zero at line center [Werner, 2005].

3.2.2.3   Pulse Length

As with DRWP systems, the pulse length sets the upper limit (highest resolution) for system resolution. Light pulses with lengths of a few to several hundred nanoseconds (~1 to ~ 100 m) are generated by the laser [Wandinger, 2005]. However, in order to improve the signal to noise ratio, typically averaging over multiple range cells is done, thus lowering the range resolution. Most applications do not require ten or even 100 meter resolution.

3.2.2.4   Power

Typical laser energy per pulse is 70 mJ with a telescope-scanner aperture of 0.45 m [Gentry et al., 2005].

3.2.3 Algorithms

The Doppler spectrum from a single beam gives the line-of-sight (radial) velocity along the beam and the horizontal wind is inferred from multiple look directions (two if the vertical velocity is assumed to be zero and a minimum of three if the vertical velocity is to be determined).

To infer the line of sight velocity, one needs to infer the center of the Doppler spectrum which has been broadened by the motion of individual scatters relative to the bulk flow. When the whole spectral distribution spectrum is obtained, such as by a high-dispersion multichannel spectrometer, the Doppler shift may be obtained by means of a Gaussian least squares fit. When a pair of filters is used (double-edge technique), the deduction involves characterizing the asymmetry induced by the Doppler shift as follows: let A be the energy received through the filter on the short-wavelength side of line center and B be the energy through the filter on the high-wavelength side. Then line-of-sight velocity v may be inferred from A and B by inverting

$$f(v) = \frac{A-B}{A+B} \qquad\qquad (3\text{-}6)$$

after background subtraction [Werner, 2005]. In addition, one must account for the contributions to A and B due a shift in the Mie peak when this peak is not negligible compared to the Rayleigh peak.

3.2.4 Current Systems

Unlike for DRWP, where there are a number of operational systems, lidar systems for launch support are under development. Here we highlight one such system, namely, the Goddard Lidar Observatory for Winds (GLOW) instrument. This is a direct detection, Doppler lidar (355 nm) that determines the velocity profiles of atmospheric molecules or particulates along the line of sight. Some systems that measure winds at lower altitude, within the boundary layer, are commercially available. See for example http://www.tpub.com/content/nasa2000/NASA-2000-cr210288/NASA-2000-cr2102880097.htm. At this writing there does not appear to be any commercially available systems that can measure winds in clear air.

3.2.4.1   GLOW Instrument Description

Velocity measurements are made using the double edge technique discussed above. The laser is a pumped Nd:YAG laser with a repetition rate of 10 Hz. The pulse length is 15 ns, and the fundamental wavelength is 1064 nm. Nonlinear harmonic generation optics produce the 355 nm pulses. The maximum laser pulse energy is typically 70-80 mJ. The backscatter laser light is collected and coupled directly to a fiber optic cable that delivers the signal to the Doppler receiver. A strength of Doppler lidars is their portability, which enables them to be moved on site to support launches. The GLOW instrument is housed in a van and is an example of a mobile direct detection system (Figure 3-6).

The molecular double edge receiver design follows the general principles described by Flesia and Korb [1999]. The collimated light from the telescope is split by beamsplitters into five channels. Two of these channels are the 'edge' channels (Figure 3-5). The third channel is used as a reference. The other two channels serve as energy monitor channels. The two edge filter channels are located symmetrically around the laser frequency in the wings of the thermally broadened molecular spectrum.

Figure 3-6. Goddard Lidar Observatory for Wind (GLOW). GLOW is a mobile Doppler lidar Rayleigh (molecular) scatter system at 355nm and an aerosol system at 1064nm [http://glow.gsfc.nasa.gov]. Image reprinted courtesy of NASA.

Photon counting Photomultiplier Tubes (PMTs) provide high detection sensitivity in the upper troposphere and stratosphere where the return signals are small. The PMT signals are sampled with a boxcar integrator and binned. Typical integration times are 30 seconds (300 shots) to 100 seconds (1000 shots) with a vertical resolution of 250 m. The laser pulse energy for these measurements is 70 mJ. The effective telescope collecting aperture is about 30 cm. The PMT's have been gated off below approximately 5 km altitude to avoid saturation.

The wind velocity can be uniquely determined by measuring the ratio of the two edge signals. The magnitude of the two edge channel signals is approximately equal at 5 km and above 20 km, but, there is a significant difference apparent between 7 and 18 km peaking at around 11 km owing to the Doppler shift due to the wind.

3.2.4.2   GLOW Performance

The GLOW Doppler lidar began atmospheric operations with the Rayleigh receiver in October 1999 and began making wind measurements in early November 1999. A validation experiment was held at the Goddard Space Flight Center that compared the lidar derived wind speed and direction with data obtained from launches of multiple radiosondes [Gentry et al., 2000]. The system was field tested for line of sight winds when GLOW was deployed to participate in the GroundWinds validation campaign held from September 18-29, 2000. In May and June of 2002 GLOW was deployed to the Southern Great Plains to participate in the International H2O Project (IHOP). GLOW was located at the Homestead profiling site in the Oklahoma panhandle. During the IHOP observation period (May 14, 2002 to June 25, 2002) more than 240 hours of wind profile measurements were obtained with GLOW.

The lidar data shown as blue diamonds in Figure 3-7 are the mean and standard deviation of three consecutive profiles of wind speed and direction taken on the afternoon of May 13, 2002. The vertical resolution of the data is 100 m and the temporal resolution is 30 minutes. Wind profile data from a radiosonde co-located at the site with GLOW is shown for comparison. Error bars indicate that the accuracy below about 8 km varies between ~1 and a few m/s, with accuracy decreasing with altitude. Above ~ 8 km accuracy decreases from a few to ~ 5 m/s near 12 km altitude. Longer integration times would give more accurate retrievals with accuracy increasing

approximately as the inverse square root of the integration time. Larger aperture-power products would also give greater accuracy.
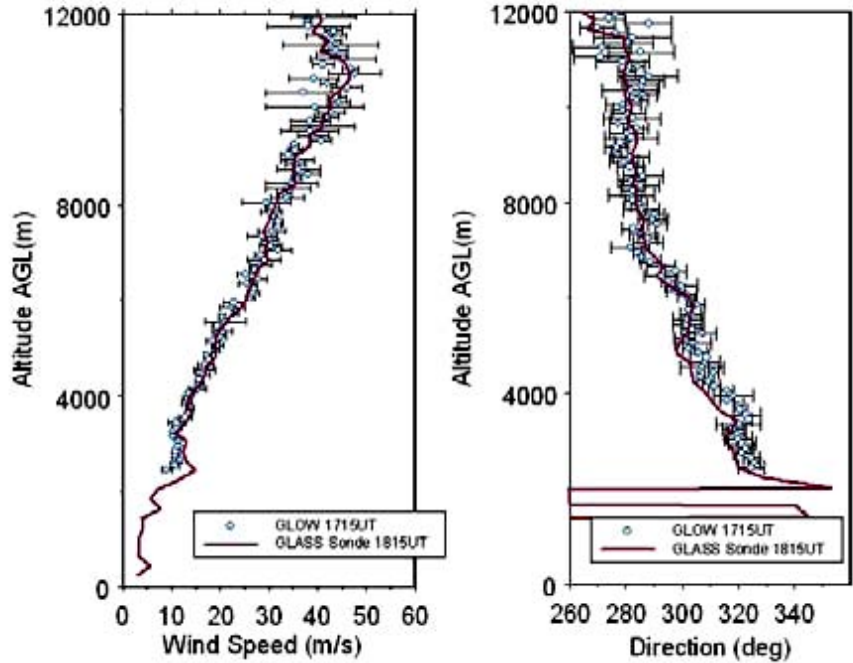
Figure 3-7. Lidar Data from May 13, 2002. The mean and standard deviation of 3 consecutive lidar profiles of wind speed (right) and direction (left) are shown (blue diamonds) along with coincident radiosonde wind data (red line). The vertical resolution of the lidar data is 100 meters [Gentry et al., 2000].

This evaluation has focused on a Rayleigh (direct detection) system because Mie systems (coherent) depend on there being sufficient aerosols concentrations. However, when aerosols concentrations are high, the coherence systems are highly accurate, ~1 m/s or better [Ishii et al., 2005]. In principle, one could operate a direct detection and coherent system at the same site to offer the advantages of both. Alternatively, hybrid systems with both direct and coherent detection have been proposed [Emmitt, 2004].

3.2.5 Strengths and Limitations

Balloon measurements suffer from the inability to provide complete profiles in less than about an hour. They do not perform measurements along the rocket trajectory and may be blown far downwind in strong winds. Both radar and lidar can complete profiles to 30 km within 30 minutes. Whereas a single lidar unit profiles winds to 30 km, a minimum of two radars operating at different frequencies are required to cover the complete altitude range. A 1 GHz UHF radar probes the 0.2 – 3 km region, a 400 MHz UHF radar is capable of interrogating 0-17 km, and a 50 MHz VHF systems covers winds the 2-20 km region. The 50 MHz radar consists of a large fixed array of antennas, whereas lidars can be mobile. Furthermore, radars do not make measurements along the vehicle trajectory. Pointing optics mounted on the lidar enclosure can direct the beam along the projected vehicle path.

The primary limitation of lidar systems is that, unlike radar, they operate at frequencies that are strongly attenuated in clouds. Lidar can penetrate only thin clouds and ground fog; rain and thick clouds will block the beam. This is mitigated by small fields of view that allow lidars to see through small gaps in the cloud cover more readily than radars. In addition, when flight is subject to lightning constraints, flight could be constrained in many cases of thick cloud cover [Krider et al., 2006].

3.3 Balloon Systems

To a good approximation, rising balloons move horizontally with the horizontal flow in which they are imbedded. Thus systems that track drifting balloons can be used to derive horizontal winds. Presently, balloons are the primary means of deducing winds for launch support.

The primary balloon systems used to support launches on the national ranges today are the radar tracked Jimsphere and Global Positioning System (GPS) tracked Automated Meteorlogical Profiling System. Balloon-tracked systems offer highly accurate high-resolution measurements. The main disadvantages to balloon systems are the time it takes to ascend to the balloon ceiling and the fact that they may be blown far down wind in high wind conditions.

3.3.1 Derivation of Winds

The information obtained by tracking systems is position data for radar-tracked balloons and both position and direct measurements of velocity with GPS-tracked balloons. Position data from radars are obtained initially in the form of range, azimuth, and elevation. It is then converted to a Cartesian x, y, z coordinate system, where x is the east-west direction (positive eastward), y is the north-south direction (positive northward) and z is the vertical direction (positive upward). To obtain winds, the position data are numerically differentiated with respect to time to give the horizontal velocity. Vertical position data from radar are not used to derive winds, but may be used as a measure of data quality. Since differentiation decreases the signal relative to the noise, measurements based on individual pairs of position data can be very noisy. Therefore, the radar data must be smoothed over layers containing a number of data points to reduce the noise to an acceptable level [Wilfong, 1997; Luers and MacArthur, 1972]. The averaging interval gives the minimum vertical resolution of the wind retrieval.

During ascent balloons are blown downwind. This means that wind-versus-altitude data do not represent the wind in a vertical column. Furthermore, the variations that are reported from one vertical position to another do not necessarily represent purely vertical variations, but can also represent horizontal variations. This is further complicated by the fact that the balloon can take an hour or more to attain the desired altitude limit. During the ascent of the balloon, temporal variations are convolved with spatial variations.

3.3.2 System Hardware

The basic elements of a balloon-based wind measurement system are the balloon and a tracker.

3.3.2.1 Balloons

Balloons are subject to aerodynamically-induced oscillations that occur as a result of interactions between the balloon and the air through which it ascends. This can be quite pronounced. Jimspheres are balloons affixed with conical projections designed to mitigate the aerodynamically

induced oscillations. For balloons that have instruments suspended below them, the motion of the balloon can also induce pendulum motion. Significant oscillations that cannot be removed by balloon designs have to be mitigated with data processing [Luers et al., 1972; Wilfong et al., 1997].

The fact that balloons can be blown far downstream during ascent means that wind measurements based on tracking in range, azimuth, and elevation can become very sensitive to errors in azimuth. For example, for flow that is primarily eastward, $v \approx r\dot{\theta}$, where r is range and θ is azimuth in radians. Under strong-wind conditions, r becomes large and small errors in θ can give large errors in the north-south wind.

3.3.2.2 Data Reduction and Quality Control

The main problems of data reduction are to reduce the variance of the estimate of wind velocity to acceptable levels and remove artifacts.

The variance is reduced by averaging tracking data through layers that contain enough data points to substantially reduce the variance of the estimates. For Jimspheres, the altitude interval is adjusted dynamically using the vertical rise rate as a quality indicator. Normally the noise level increases with altitude, especially in strong-wind conditions.

Tracking data may be subject to artifacts that cannot be removed by data processing. For radar-tracked balloons this includes acquisition of the balloon by side lobes rather than the main lobe and loss of track. The effects of these anomalies can be severe. Thus, manual quality control is required to identify and, if possible, solve the problem. With manual QC, these problems can be often be identified and solved in real time, either by notifying the operator or by editing the data by hand.

3.3.3 Operational Systems

3.3.3.1 Radar-tracked Jimsphere

The radar-tracked Jimsphere has been the benchmark for high resolution wind measurements in support of launches for the last 35 years. The balloon is a 2 m diameter sphere with ~ 400 cones attached, each approximately 0.08 m high. Before inflation the mass of the system is 0.41 kg [Wilfong et al., 1997]. The rise rate of the Jimsphere varies linearly between 5.4 m s^{-1} at sea level and 4.5 m s^{-1} at 15 km, where a more rapid slowing in rise rate commences; reaching its nominal ceiling of around 17 km in about an hour [Wilfong et al., 1997].

The Jimsphere is designed to reduce spurious, self-induced balloon oscillations. The design produces a controlled self induced-oscillation with period of 4.7 s that can be removed from the tracking data [Wilfong et al., 1997; check paper for details].

It is possible to use any range radar, but normally Jimsphere tracking at the Eastern and Western ranges is done with an AN/FPS-16 radar. Performance specifications give nominal rms noise errors of 4.5 m in range and 10^{-4} radians in azimuth and elevation, but performance may vary among different operation procedures [Luers and MacArthur , 1972; Wilfong et al., 1997].

The Rose program converts radar tracking data into a wind profile. Data are normally acquired at a rate of 10 Hz. The wind computation begins with 100-ft layers. The Rose program then attempts to maintain a precision of 1 m s^{-1} in each component by adjusting the averaging layer as the noise

level increases, as indicated by the standard deviation of the rise rate [Wilfong et al., 1997]. The layer depth is increased in 100-ft increments up to 400 ft (121.9 m). Figure 3-8 shows the average magnitude of the wind vector error as a function of altitude as determined from 33 dual tracked Jimspheres. The smoothed plot is a polynomial fit. Errors are generally less than 0.5 m/s below 10 km, increasing to ~ 0.7 m/s by 15 km.
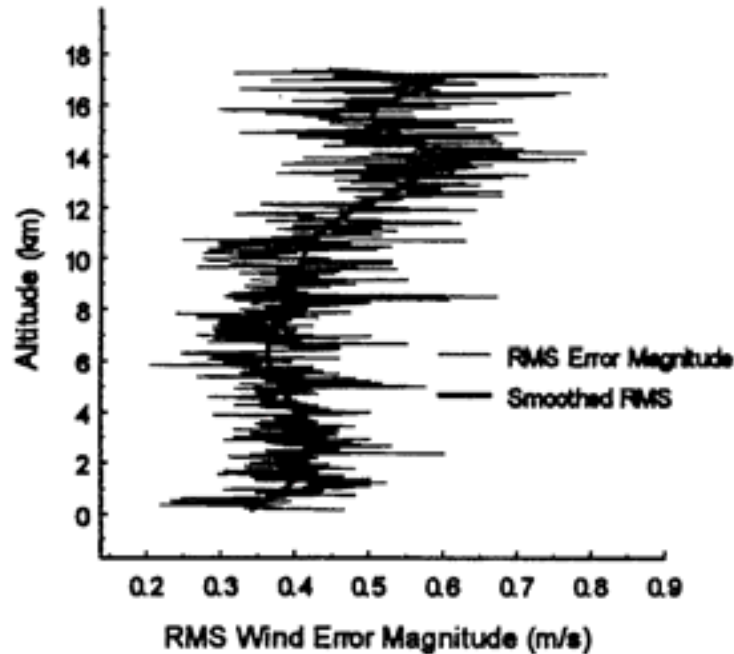
Figure 3-8. Average Magnitude of the Wind Vector Error as a Function of Altitude as Determined from 33 Dual Tracked Jimspheres. The smoothed plot is a polynomial fit [Wilfong et al, 1997].

3.3.3.2 Automated Meteorological Profiling System (AMPS)

The AMPS system uses the GPS to obtain profiles of wind velocities. AMPS utilizes Differential GPS (DGPS) technology to provide accurate, high-resolution profiles of wind up to 30 km. AMPS was initially developed for the United States Air Force to provide upper air data at the Eastern and Western Ranges [ERIH, 2007].

The AMPS system consists of two major elements, a Ground Element (GE) and a Flight Element (FE). The GE controls the preparation of the FE for flight and receives the radio frequency (RF) data stream from the FE during flight, which is then converted to the required atmospheric parameters. The GE generates time and altitude sequenced listings of the required atmospheric parameters for up to six FEs at a time and transfers these data to an external processing and display system.

AMPS flight elements are available in two configurations, a High Resolution Flight Element (HRFE) and a Low Resolution Flight Element (LRFE). The HRFE is a replacement for the radar tracked Jimsphere system at Cape Canaveral Air Force Station (CCAFS) and consists of a Global Positioning System (GPS) radiosonde attached to a clear Jimsphere balloon and is solely used to produce high-resolution measurement of wind with respect to altitude. The LRFE consists of a standard helium-filled latex meteorological balloon, which lifts a radiosonde containing a

miniaturized GPS receiver, a radio transmitter, meteorological sensors, and a battery. The HRFE prepared for release is shown in Figure 3-9. Data processing provides vertical profiles wind from the surface to near 35 km (100,000 ft) [ERIH, 2007; Leahy, 2004].

The HRFE rawinsonde (radiosonde that also measures wind) provides only wind data at 30.5 m intervals from the surface up to 17 km, and was designed to provide the same high-resolution wind data as the radar-tracked Jimsphere. The clear Jimsphere balloon prevents the HR rawinsonde from ascending higher than 17 km [ERIH, 2007]

Each GE consists of a set of three external antennas, with associated preamplifiers, mounted atop a 30 ft tower located adjacent to the Weather Station building, and a System Computer, the AMPS system software, and an equipment cabinet containing six Signal Processing Subsystems (SPSs), all located inside the Weather Station [ERIH, 2007].

At the Eastern Range AMPS balloons run several hundred dollars each counting the balloon, sonde, helium and labor [Dr Merceret, Applied Meteorological Unit, KSC].

3.3.3.3 Data Reduction

The Wind Finding program consists of a Kalman filter tuned to estimate horizontal winds and altitude for the AMPS-specific HR rawinsonde and LR rawinsonde using data from the ground element base receiver and the radiosonde on-board GPS receiver. The Wind Finding program also includes a notch filter for the HR rawinsonde wind data and a 44th Order Finite Impulse Response (FIR) filter for the LR rawinsonde data. The filter has resulted in producing LR rawinsonde wind profiles that are comparable to the profiles generated from the AMPS HR rawinsonde and radar-tracked Jimspheres. The Kalman filter uses data from the System Computer, the rawinsonde's GPS receiver, and SPS Base DGPS receiver to estimate the rawinsonde's navigation solution and wind velocities [ERIH, 2007].

Figure 3-9. Jimsphere Balloon Used for High Resolution Wind Measurements
[Fig. 1, Decker and Leach, 2004. Image reprinted with permission of authors.]

3.3.4   Strengths and Limitations

Balloon measurements are the standard for wind measurements. The drift of the balloons closely reflects the winds. The balloons are tracked with great precision and accuracy.

The biggest drawback to the balloon systems is the fact that they rely on the rising drifting balloon to sense winds. It takes an hour for a balloon to reach altitudes near 18 km. In addition to introducing delays and uncertainties in the wind profile because of temporal changes in the winds, the balloon may drift 100 km or more away from the launch site. In rapidly changing situations, these factors can introduce large differences between the wind at the balloon location and the wind at the launch site [Schumann et al., 1994, Wilfong et al., 1993a].

4. Extension of DRWP Altitude Coverage

[The material in this section was provided by personal communication with Dr. Francis Merceret, Applied Meteorological Unit, KSC, Florida].

Before the KSC 50 MHz instrument was taken operational using the improved signal processing now used for operational support, it used the standard "consensus" signal processing. When operating on that software, it could operate in either of two modes. "Low mode" had the same spatial properties as the current operational system (2 to 18 km at a gate spacing of 150m), although the consensus could only produce two profiles per hour, and the quality was not as good as the current system (which as configured produces 12 profiles per hour and is capable of nearly 20 per hour). The other mode was "high mode" which produced profiles from 20 to 90 km with a gate spacing of 600m. The KSC experience with that was limited and not very encouraging (which is part of the reason it remained limited).

The problem is that the effective radar scattering coefficient of the atmosphere increases with two variables: humidity and turbulence level. Both become quite small in the stratosphere. It was found that on most days, high mode signal-to-noise ratios (SNRs) were too small to produce a valid profile using the consensus method except in the regions of breaking internal gravity waves if and when they occurred.

No attempt was made using the present algorithm in high mode – it was not coded to handle the 600m gate spacing. It could improve the performance substantially when a signal is present, but it cannot manufacture a signal when none is detectable. There are four ways to improve the SNR given the state of the atmosphere: increase the aperture, increase the power, increase the vertical averaging interval (gate spacing and pulse length), and increase the integration time (time between profiles). Improved signal processing, of course, would also help. The best proven signal processing for operational profilers is the one used (Median Filter-First Guess, MFFG).

Most VHF profilers operating elsewhere in the 40 - 60 MHz region operate primarily from 2 to 20 km altitude with 150 to 600 m gate spacing using a consensus-type algorithm to produce profiles at 30 minute to 1 hour intervals. A few are configured for mesospheric-stratospheric operations with larger gate spacing and longer averaging times, but many mesospheric wind-finding radars use meteor scatter techniques rather than the index of refraction fluctuation scattering used by tropospheric radars because that's the only way to get enough signal reliably. Both the radar and the software are configured quite differently for that methodology.

Dr. Merceret believes that a VHF profiler in the 40 - 60 MHz range (lower is better) could be configured to work to 150 kft (45 km) provided that it uses software at least as good as the MFFG algorithm, rather than consensus, and goes to 1km gate spacing with the integration time from 30 minutes minimum to as much as an hour. The power-aperture product would also have to be at least as large as the present KSC system with a physical aperture of about 15,000 square meters and a peak power of 250 KW. This is not enough with a 600m gate spacing and half-hour consensus in high mode. In low mode with the MFFG, power is routinely reduced to near 100 KW to increase the service life of the system and still have more than adequate SNR.

5. Reliability

Data for 50 MHz profiler reliability for 2008 were provided by Dr. F Merceret (Applied Meteorological Unit, Kennedy Space Center, Florida) courtesy of Bill Gober of BAE Systems. The data are summarized as follows:

- Total outages (planned and unplanned) due to the profiler: 9.3%

- Total outages due to utilities: 3.0%

- Unique air conditioning (AC) downtime: 5.4%

- Profiler availability (exclusive of AC failure): 90.7%

- Data availability (exclusive of AC failure): 87.7%

- Data availability (all inclusive): 82.3%

Note: The AC failure data is non-representative because the majority of down time hours were related to contractual issues.

A reliability analysis of the high resolution AMPS Flight Element (HRFE) and Jimsphere based on Space Shuttle Program (SSP) Launch and Landing Program Requirements Document (PRD) requirements (Item HT17E) was performed by Marshall Space Flight Center (MSFC) (Briefing charts by Ryan Decker/MSFC/EV44, March 23, 2009) and provided by Dr. F. Merceret. The PRD requirements are

- Data acquisition before 1500 ft.

- Data to at least 52000 ft.

- Must reach 52000 ft within 60 minutes.

- No data interpolations greater than 400 ft from 1500-52000 ft. Interpolations in HRFE are due to either missing or noisy data.

- Interpolations in Jimsphere are primarily due to either radar handoff errors or loss of radar track.

- Reliability of the system must be at least 95%.

The HRFE data analyzed were 209 profiles between January 2006 and February 2009 and 106 HRFE profiles between January 2006 and February 2009. Profiles were gathered from AMPS testing, SSP launches and launch simulations and ELV launches and launch simulations. The Jimsphere data analyzed were 88 Jimsphere profiles between April 2005 and February 2009 and 102 Jimsphere profiles between April 2005 and February 2007. The profiles were gathered from SSP launches and simulations. The HRFE reliability was found to be 88% and the Jimsphere reliability 83%.

6.   Wind Modeling

First-principles dynamical modes have been developed that have considerable forecasting skill. The most promising of these are the mesoscale models with their high resolution and the ability to include local influences such as topography and surface conditions (e.g., land usage, snow cover, wetness). This section will dwell on these models, including especially the recently implemented Weather Research and Forecasting (WRF) system.

6.1   Numerical Weather Prediction Models

Numerical weather prediction (NWP) models solve the fluid equations for the atmosphere by approximating the continuous form of the equations with derivatives evaluated on a grid. Historically, operational NWP models have been rather coarse gridded with typical grid spacing of 5 degrees in latitude and longitude. For middle latitudes this gives grid spacing of ~ 500 km (300 miles). These models were suitable for influences that affect winds on synoptic scales (a few thousand kilometers), but are too coarse to account for important local effects that can influence the winds at a given site. In recent years a number of sub-synoptic-scale models have been developed that account for influences with scales of tens of kilometers and less. These are mesoscale models.

6.2   Mesoscale Models

Mesoscale models because of their high resolution are typically not global models. Instead they have limited area grids that may be relocated optimally for a given site or area. Some models have nested domains that have finer resolution for the inner domains than for the outer. Vertical resolution may be variable as well, with finer resolution near the ground than in the upper levels. While the resolution is finer than for typical global models, it is not fine enough to resolve all relevant processes, such as individual convective cells (e.g., thunderstorms) or turbulent eddies (along with turbulent fluxes); for these processes recourse must be made to parameterizations [Pielke and Pearce, 1994]. The following sections focus on two mesoscale models: Mesoscale Model Version 5 (MM5), which is in wide use and has a large community of users, and the Weather Research Forecast model developed in recent years for a wide range of applications, from research to operational forecasting, with priority emphasis on horizontal grids of 1–10 kilometers. Verification statistics for these models are given in graphical form in Appendix A for a number of sites in the southwestern United States; these data supplement the data given in the following sections.

6.2.1   Mesoscale Model 5 (MM5)

One mesoscale model in particular has been in wide use in recent years, the Mesoscale Model 5 (MM5) where 5 refers to the generation number. This model was co-developed by Pennsylvania State University (Penn State) and the National Center for Atmospheric Research (NCAR) [Grell et al., 1995; Anthes and Warner, 1978; Anthes et al. 1987]. Because this model is widely used and is readily available, statistics for the accuracy of this model are given. The MM5 has been continuously improved by contributions from users at universities and government laboratories [Anthes, 1972, 1977; Anthes and Warner, 1978; Anthes et al., 1987; http://www.mmm.ucar.edu/mm5/overview.html].

The MM5 mesoscale model is a limited-area, nonhydrostatic, terrain-following sigma-coordinate model designed to simulate or predict mesoscale and regional-scale atmospheric circulation. The vertical σ-coordinate is defined in terms of pressure as

$$\sigma = \frac{p - p_t}{p_s - p_t} \qquad\qquad (6\text{-}1)$$

where p_s and p_t are the surface and top pressures respectively of the model and where p_t is a constant [Grell et al., 1995]. Sigma surfaces near the ground closely follow the terrain, and the higher-level sigma surfaces tend to approximate isobaric surfaces.

The MM5 model is the latest in a series that developed from a mesoscale model used at Penn State in the early 1970's [Anthes and Warner, 1978]. Since that time, it has undergone many changes designed to broaden its usage. These include:

- A multiple-nest capability where grids of higher resolution are contained within coarser grids

- Non-hydrostatic dynamics, which allows the model to be used at a few-kilometer scale

- A four-dimensional data-assimilation capability that allows new observations to be brought in more or less continuously

- More physics options (e.g., boundary layer schemes)

The model is supported by several auxiliary programs, which are referred to collectively as the MM5 modeling system. Documentation for various programs in the modeling system is available online [see Documents and Publications in the link http://www.mmm.ucar.edu/mm5/overview.html].

Meteorological data are horizontally interpolated from a latitude-longitude mesh to a variable high-resolution domain on a Mercator, Lambert conformal, or polar stereographic projection. Since the interpolation does not provide mesoscale detail, the interpolated data may be enhanced with observations from the standard network of surface and rawinsonde stations [Grell et al., 1995]. A vertical interpolation is performed from pressure levels to the sigma coordinate system defined above.

The vertical and horizontal resolution and domain size are variable. Since MM5 is a regional model, it requires an initial condition as well as lateral boundary conditions to run. The lateral boundary condition is interpolated from the output of a larger-scale model and involves relaxing" or "nudging" the model predicted variables toward a large-scale analysis. To produce lateral boundary condition for a model run, one needs gridded data to cover the entire time period that the model is integrated. The model employs a sponge upper boundary condition to prevent the spurious reflection of wave energy from the upper boundary [Grell et al, 1995; Klemp and Durran, 1983; Bougeault 1983; http://www.mmm.ucar.edu/mm5/overview.html].

Table 6-1 shows 24-hour forecast verification statistics for winds speed for various sites in the southwestern United States [data were provided by Mr. Robert Craig, Air Force Weather Agency, Offutt AFB, NB]. Model data are compared to winds from standard metrological soundings

(rawinsondes). The data are the root-mean-square errors and biases for the wind magnitude (speed) at various sites. The data are given in knots (1 knot = 0.5144 m/s). The data cover the approximate altitude range from 9.7 to 21 km, and are thus indicative of the winds in the upper troposphere and lower stratosphere. Generally, the bias is small, being less than ~ 1 m/s for altitudes at and below 16 km. For 21 km the biases increase to ~ 4-7 m/s. The variation between locations is not great indicating the model accuracy at these altitudes is not overly sensitive to local conditions. Values of RMS error lie between ~ 3 and 5 m/s, except for El Paso, where errors are significantly less.

Tables 6-2 and 6-3 show 24-hour forecast error statistics (bias and RMS) for the u and v wind components at Vandenberg AFB (WR) during a spring and summer season, respectively. The statistics are based on predictions with the MM5 and WRF models hosted by The Aerospace Corporation and once daily radiosonde data from Vandenberg AFB. Data are shown for various layers from the surface to 100 mb (~ 16 km or 50,000 ft). The spring data (Table 6-2) show small biases (less than ~ 1 m/s in magnitude) except for the u component above 500 mb, where the bias is -1.4 m/s. The RMS values for both components do not vary much below 500 mb and are less that ~ 4 m/s. Above 500 mb the RMS errors for both components increase to ~ 5 m/s. The summer data (Table 6-3) show somewhat smaller errors, probably indicative of weaker winds in this season.

6.2.2   Weather and Research Forecast (WRF) Model

The new generation WRF model was developed through a collaborative partnership, principally among the National Center for Atmospheric Research (NCAR), the National Oceanic and Atmospheric Administration's (NOAA's) National Centers for Environmental Prediction (NCEP), the Forecast Systems Laboratory, the Air Force Weather Agency (AFWA), the Naval Research Laboratory, Oklahoma University, and the Federal Aviation Administration (FAA) [http://www.wrf-model.org/index.php]. The WRF system is in the public domain and is freely available. It is designed to be efficient on available parallel computing platforms [http://www.mmm.ucar.edu/wrf/users/].

Table 6-1. MM5 24-Hour Verification Statistics for Wind Speed for Various Sites at
Various Pressure Altitudes in the Southwestern US

Station Name	Block Station #	250mb RMSE Bias		200mb RMSE Bias		150mb RMSE Bias		100mb RMSE Bias		50mb RMSE Bias	
DFW TX	722490	7.4	0.2	7.4	0.2	8.8	0.0	8.7	0.7	14.0	-11.9
Midland TX	722650	6.8	-0.5	6.8	-0.5	8.2	-1.5	7.0	-1.8	14.6	-13.0
Tucson AZ	722740	6.4	0.3	6.4	0.3	6.6	-2.2	8.0	-3.1	14.5	-12.5
San Diego CA	722930	7.0	-0.8	7.0	-0.8	7.0	-2.0	6.1	-1.3	12.7	-10.7
Oklahoma City OK	723570	8.3	-0.2	8.3	-0.2	8.6	0.2	8.3	-0.7	11.1	-8.1
Amarillo TX	723630	8.4	0.2	8.4	0.2	9.0	-2.5	7.0	-2.9	11.8	-8.0
El Paso TX	723640	4.8	0.6	4.8	0.6	6.4	-1.6	7.3	-2.6	16.8	-14.9
Albuquerque NM	723650	7.0	0.0	7.0	0.0	7.2	-0.9	7.6	-1.3	12.1	-8.6
Flag Staff AZ	723760	9.5	2.3	9.5	2.3	10.9	0.9	9.8	-1.1	11.7	-8.1

The data are the root-mean-square errors and biases for various sites. Model data are compared to winds from standard metrological soundings (rawinsondes). The data are given in knots (1 knot = 0.5144 m/s). Other conversions are 1mb = 1hPa, and the following approximate altitudes correspond to the indicated pressure levels: 250 mb = 9.7 km, 200 mb = 11.3 km, 150 mb = 13.3 km, 100 mb = 16.1 km and 50 mb = 21.0 km. These data were provided by Mr. Robert Craig of the Air Force Weather Agency, Offutt AFB, NB.

Table 6-2. Wind Verification Statistics for MM5 24-hour Forecasts for
Vandenberg AFB, CA

	MM5 24-hour Forecast			
	U Comp (m/s)		V Comp (m/s)	
level	Bias	RMS	Bias	RMS
surface - 850	-0.64	3.21	-0.33	3.21
850 mb - 500	-0.16	2.63	0.95	2.97
500 mb - 700	-0.87	3.32	-0.28	3.82
100 mb - 500	-1.38	4.69	-1.05	4.62

Data are for March 19 to May 31, 2008.

Table 6-3. Wind Verification Statistics for MM5 24-hour Forecasts for Vandenberg AFB, CA

	MM5 24-hour Forecast			
	U Comp (m/s)		V Comp (m/s)	
level	Bias	RMS	Bias	RMS
surface - 850	0.55	2.59	-0.96	3.15
850 mb - 500	-0.20	2.57	-0.66	3.20
500 mb - 700	-0.36	3.62	-0.50	3.97
100 mb - 500	-0.60	3.88	-2.01	4.59

Data are for June 1 to August 6, 2008.

Table 6-4. Wind Verification Statistics for WRF 6-hour Forecasts for Vandenberg AFB, CA

	Six Hour WRF Forecast			
	U Comp (m/s)		V Comp (m/s)	
Layer (mb)	Bias	RMS	Bias	RMS
surface - 850	-0.19	2.94	-0.36	3.36
850 - 700 mb	0.02	2.74	0.38	3.37
700 - 500 mb	-0.38	3.15	-0.80	3.38
500 - 100 mb	-0.60	3.71	-1.51	4.05

Data are for March 19 to May 31, 2008.

This model incorporates advanced numerics and data assimilation techniques, a multiple relocatable nesting capability, and improved physics, particularly for treatment of convection and mesoscale precipitation. It is intended for a wide range of applications, from idealized research to operational forecasting, with priority emphasis on horizontal grids of 1–10 kilometers [Michalakes et al., 2001]. The WRF model has been deployed for operational use, notably by NCEP and AFWA. However, the version used by NCEP has a different physical core (different numerics) than the version in use elsewhere [http://www.dtcenter.org/wrf-nmm/users/]. The NCEP version is the WRF-Nonhydrostatic Mesoscale Model (WRF-NMM). The version used by NCAR and AFWA is the Advanced Research WRF (WRF-ARW).

Table 6-4 shows verification statistics for six-hour forecast for the individual wind components for Vandenberg AFB for various layers from the surface to 100 mb (~ 16 km or 50,000 ft). The data are for the 2008 spring period March 19 – May 31. Model data are compared to winds from the metrological soundings from Vandenberg AFB. The data for the u component show little bias (less than 1 m/s in magnitude). The RMS values vary from ~3 m/s to values near 4 m/s, with an overall tendency to increase with altitude. For the v component the same trends are seen, but the bias in the layer above 500 mb is significantly larger (-1.5 m/s).

Table 6-5 is the same as 6-3 except for 24-hour forecasts. Biases are similar, being generally less than 1 m/s in magnitude for both components. The exception is a bias of 1.4 m/s for the v component for the layer from 850-700 mb. The RMS errors are larger than for the 6 hour forecast, but the difference is not large. Errors are largest in the uppermost layer where values of ~4.8 m/s are attained.

Tables 6-6 and 6-7 are the same as Tables 6-4 and 6-5, respectively, except for the 2008 summer season, June 1 – August 6. The statistics are similar to those for the spring period except for

larger biases for the v component in the lowest layer (magnitude >1 m/s) and uppermost layer (magnitude > 2 m/s).

Table 6-5. Wind Verification Statistics for WRF 24-hour Forecasts for
Vandenberg AFB, CA

| level | WRF 24-hour Forecast | | | |
| | U Comp (m/s) | | V Comp (m/s) | |
	Bias	RMS	Bias	RMS
surface - 850	-0.08	3.30	-0.69	3.33
850 mb - 500	0.75	2.76	1.36	3.56
500 mb - 700	-0.18	3.32	-0.19	4.13
100 mb - 500	-0.24	4.76	-1.02	4.64

Data are for March 19 to May 31, 2008.

Table 6-6. Wind Verification Statistics for WRF 6-hour Forecasts for
Vandenberg AFB, CA

| Layer (mb) | WRF Six Hour Forecast | | | |
| | U Comp (m/s) | | V Comp (m/s) | |
	Bias	RMS	Bias	RMS
surface - 850	-0.05	2.46	-1.19	3.46
850 - 700 mb	0.10	2.90	-0.24	2.39
700 - 500 mb	0.31	2.54	-0.52	2.93
500 - 100 mb	0.59	3.23	-2.34	3.81

Data are for June 1 to August 6, 2008.

Table 6-7. Wind Verification Statistics for WRF 24-hour Forecasts for
Vandenberg AFB, CA

| level | WRF 24 Hour Forecast | | | |
| | U Comp (m/s) | | V Comp (m/s) | |
	Bias	RMS	Bias	RMS
surface - 850	0.64	2.73	-1.38	3.35
850 mb - 500	0.51	2.58	-0.59	3.47
500 mb - 700	0.36	3.46	-0.77	3.82
100 mb - 500	0.48	4.00	-2.05	4.62

Data are for June 1 to August 6, 2008.
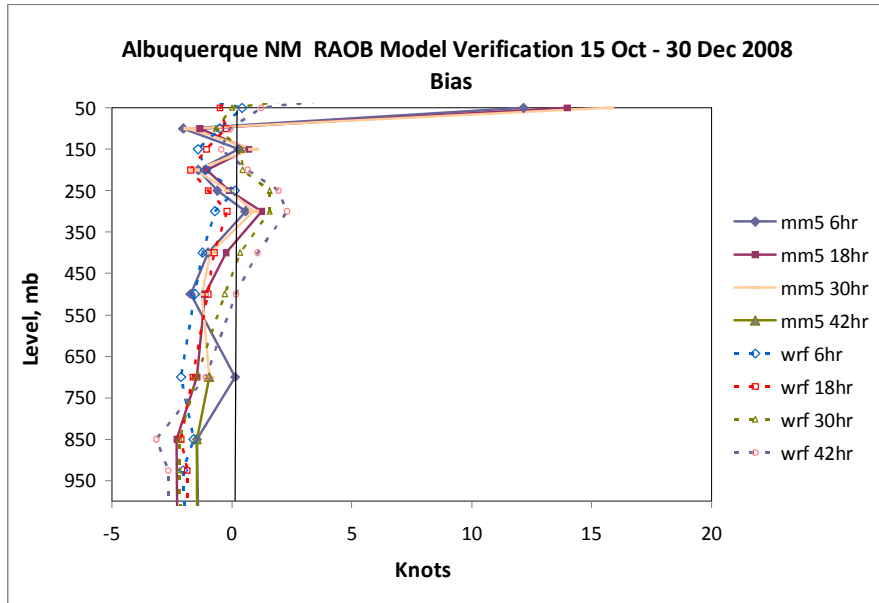
Figure 6-1. Wind Speed Bias for Albuquerque, New Mexico.

The data shown in the preceding section indicate the performance of the two models is similar. This is illustrated in Figure 6-1. This figure shows wind speed bias for the two models for a fall season. The biases are of similar magnitude for altitudes below 100 mb. Above 100 mb the bias for the WRF model is markedly better. The MM5 upper boundary is at 50 mb for these runs and this is the most likely cause of the degraded forecasts for this model.

Despite the near parity in present accuracy, the WRF model is still in its formative stages and should improve. The MM5 is no longer supported by annual user meeting at the National Center for Atmospheric Research (NCAR) and the pace of future improvements will most likely be limited.

7. System-by-System Wind Technology Comparisons

The nominal performance of the three primary systems used to support launch activities are shown in Table 7-1. The advantages and disadvantages of each system are also summarized.

Table 7-1. Summary of System Capabilities

	Type	Range (km)	Vertical Resolution (m)	Bias (m/s)	Precision (m/s)	Advantages	Disadvantages
Balloon (1,2,3)	AMPS High Res	17	160	≤ 0.7	0.6	Highest accuracy and vertical resolution. All weather.	May take ~ hour or more to retrieve entire profile. Balloon may drift 10s of kilometers during ascent. For radar-tracked balloons drop out and sideband acquisition may occur
	AMPS Low Res	33	350	0.7	1.0		
	Jimsphere	17	100-300	≤ 0.7	0.5 + 1% of layer wind speed		
Doppler Radar (1,4,5, 6,7)	50 MHz	20	500	0.1	1.5	Good accuracy and resolution. All weather. Good temporal resolution. Retrievals for wind overhead	Not mobile. Subject to ground clutter, sideband ambiguities and spurious reflections. Dropout due to low signal (weak turbulence) may occur.
	UHF	5 (915 MHz) - 14 (404 MHz)	----	<1.7	1.7		
Lidar (8)	GLOW	25	200	---	3 up to ~ 12 km altitude	Good accuracy and resolution. Good temporal resolution. Retrievals for wind overhead. Easier to locate near launch site.	Not all weather. Technology not as mature and performance is not as well characterized. Requires periodic calibration.
Mesoscale Models	MM5 (AFWA)	20 (50 hPa)	Config-urable	1	5	Inexpensive. Can be run from one location for arbitrary site.	Subject to model biases for different locations (forecast mode). Less accurate than collocated observations.
	WRF (AFWA)	32 (10 hPa)	Config-urable	1	5		

(1) ERIH, 2007; (2) Leahy, 2004; (3) Wilfong et al, 1997; (4) Printer et al., 2006; (5) Merceret, 1999; (6) Frisch et al., 1986; (7) Strauch et al., 1987; (8) Gentry et al., 2000

Table 7-2 Summary of the vertical range of the systems considered in this report in both metric and English units

Table 7-2. Summary of Approximate Vertical Coverage for Various Systems

Method	Peak Altitude Capability (km)	Peak Altitude Capability (ft)
Doppler radar	20	65,000
Doppler lidar	25	82,000
Jimsphere	17	56,000
AMPS (High res)	17	56,000
AMPS (Low res)	33	108,000
WRF model	32*	105,000*

*Configurable: The basic limitation is the altitude coverage of the data used to initialize the model, up to ~ 32 km (105,000 ft) in practice).

8. Recommendations

Three measurement systems (balloon, radar and lidar) have been examined and characterized. In addition numerical weather prediction models have been reviewed. Each system has its advantages and disadvantages. In terms of performance alone there is little to choose between balloons, radar and lidar. In terms of accuracy and vertical resolution balloons offer the best performance. However, it takes approximately an hour or more for balloons to reach their limiting altitude and in that time balloons can drift to distances approaching 100 km. This occurs when winds are strongest and are most likely to an operational factor. There is a limitation on how many Balloons can be tracked and processed simultaneously and this limits the time resolution. For single balloon tracking the time resolution is limited to an hour or so and during this time large changes in the wind can occur. Doppler radar profilers are less accurate and have poorer resolution but are nonetheless likely to be sufficiently accurate for operational purposes. They offer the important advantage that the measured winds are overhead and comparatively timely. Lidar has similar advantages to radar profilers, but lacks an all weather capability. However, several commercial launch sites are in locations with rather dry climates and days with severe attenuation may occur comparatively seldom. In addition, Reusable Launch Vehicle launches may be subject to lightning flight rules that could already constrain launches when there is significant cloudiness [Krider et al., 2006]. Numerical weather prediction models are less accurate than on site measurements but can be produced for a particular site and can be used to anticipate changes.

The precise system performance (accuracy, precision, reliability) required to support RLV flights is not known. Clearly, since balloon systems support launches of large expendable launch vehicles and the Space Shuttle they would be accurate and dependable enough to support RLV launches. Since the performance of the large powerful radars such as the ER and WR 50 MHz radars these most likely would also be adequate. Less certain is the adequacy of less capable radars, lidars and numerical weather prediction.

Balloon systems and the most capable of radar systems should be adequate stand alone systems. Both are accurate, reliable and essentially all-weather. The best balloon solution would be one based on GPS. This alleviates the need for expensive high precision tracking by radar. At present there are no operational Doppler lidars. However, lidars offer the advantage of mobility. Future lidars should provide a good solution for locations that are not limited by layered cloud when lightning constraints allow flight.

The safest system would be a remote measurement system (radar or lidar) in combination with a balloon system. This system would be robust and would offer the accuracy, precision and reliability of the balloon system with the timeliness and localized sampling of a radar or lidar.

Numerical weather prediction is less accurate than measurements, but in the absence of accuracy criteria for RLVs its utility as a means for assessing wind effects cannot be ruled out. Whether NWP as a standalone system is adequate depends on the sensitivities of the vehicle and the control requirements. At a minimum, the accuracy of the model predictions is a great improvement over climatology. Models can be employed to provide situational awareness. They would provide a good indication that present conditions will not persist. They will also provide an understanding of the causes of changes in the weather that are being experienced and how long unsettled conditions might persist.

9. Summary

The principles and the operational characteristics of balloon and radar-based techniques for measuring upper air winds in support of launches and recoveries have been presented. Each technique has advantages and disadvantages. The most effective approach to meeting upper air wind requirements may involve a mixed set of instruments, each with different strengths.

Balloon-based systems tend to have finer spatial (vertical) resolution than radar-based ones, whereas the radar-based systems have finer temporal resolution. The two kinds of systems appear to have approximately equal accuracy and reliability. As implemented at the Eastern Range, the QC latencies for balloon- and radar-based systems are each about 5 minutes. The radar profilers scan a fixed vertical volume whereas balloons drift with the wind. The volume of the latter sample is neither constant from profile to profile, nor is the volume overhead.

The best mix for generating high-quality wind profiles may consist of a DRWP in combination with balloons. The former gives more timely observations in a fixed volume, while the latter provide higher resolution.

10. References

Anthes, R. A., The development of asymmetries in a three-dimensional numerical model of the tropical cyclone. Mon. Wea. Rev., 100, 461-476, 1972.

Anthes, R. A., A cumulus parameterization scheme utilizing a one-dimensional cloud model. Mon. Wea. Rev., 105, 270-286, 1977.

Anthes, R. A., and T. T. Warner, Development of hydrodynamic models suitable for air pollution and other mesometeorological studies. Mon. Wea. Rev., 106, 1045-1078, 1978.

Anthes, R. A., E.-Y. Hsie, and Y.H. Kuo, Description of the Penn State/NCAR Mesoscale Model Version 4 (MM4). NCAR/TN-282+STR, National Center for Atmospheric Research, Boulder, CO, 66 pp., 1987.

Baker et al., Measured winds from space: A key component for weather and climate prediction, Bull. Amer. Meteor. Soc., 76, 1995.

Bowdle, D. A, A global-scale model of aerosol backscatter at CO_2 wavelengths for satellite-based lidar sensors. Preprints, Second Cont. on Satellite Meteorology/Remote Sensing and Applications, Williamsburg, VA, Amer. Meteor. Soc., 303306, 1986.

Barth, M. F., R. B. Chadwick and D. W. van de Kamp, Data processing algorithms used by NOAA's wind profiler demonstration network, Ann. Geophysicae, 12, 518-528, 1994.

Beran, D. W., and T. L. Wilfong, U. S. Wind Profilers: A Review, Federal Coordinator For Meteorological Services And Supporting Research, FCM-R14-1998, 1998.

Birkemeier, W. P., H. S. Merrill Jr.; D. H. Sargeant; D.W. Thomson; C. M. Beamer; G.T Bergemann, Observation of wind-produced Doppler shifts in tropospheric scatter propagation. Radio Science, 3, 309, 1968.

Bougeault, P., A non-reflective upper boundary condition for limited-height hydrostatic models. Mon. Wea. Rev., 111, 420-429, 1983.

Brode, R., (Ed.), Meteorological Monitoring Guidance for Regulatory Modeling Applications, Environmental Protection Agency, EPA-454/R-99-005, February 2000.

Byron Edde, Radar: Principles, Technology, Applications, Prentice Hall Professional Technical Reference, ISBN-13: 9780137523467, 816pp, 1992.

Coulter, R., Radar Wind Profiler and RASS (RWP50) Handbook, ARM TR-045, Work supported by the U.S. Department of Energy, Office of Science, Office of Biological and Environmental Research, 2004.

Decker, R. K., and R. Leach, Tropospheric wind monitoring during day-of-launch operations for National Aeronautics and Space Administration's Space Shuttle program, 11th Conference on Aviation, Range and Aerospace, American Meteorological Society, Hyannis, MA, Oct. 3-8, 2004.

Ecklund W.L., Carter D.A., and Balsley B.B. A UHF wind profiler for the boundary layer: brief description and initial results. J. Atmos. Ocean. Technol., 5, 432-441, 1987.

Emmitt, G. D., Combining direct and coherent detection for Doppler wind lidar, Laser Radar Techniques for Atmospheric Sensing, U. N. Singh (Ed.), Proc. SPIE, 5575, 31-37, 2004.

ERIH, Eastern Range Instrumentation Handbook, Computer Sciences Raytheon, CDRL A209, Prepared for 45th RMS/RMOE, Patrick AFB, Contract F08650-00-C005, 2007.

Fischler, M. A., and J. C. Bowles, A random sample consensus: A paradigm for model fitting with applications to image analysis and automated cartography. Commun. Assoc. Comput. Mach., 224, 381–395, 1981.

Flesia, Cristina, and C. L. Korb, Theory of the double-edge molecular technique for Doppler lidar wind measurement, Applied Optics, 38, 432-440, 1999.

Grell, G. A, J. Dudhia, D. R. Stauffer, A Description of the Fifth-Generation Penn State/NCAR Mesoscale Model (MM5), NCAR Technical Note NCAR/TN-398 + STR, 1995.

Gentry, B. M. H. Chen, S. X. Li, Wind measurements with 355-nm molecular Doppler lidar, Optics Letters, 25, 1231-1233, 2000.

Gentry, B., H. Chen, Profiling tropospheric winds with the Goddard Lidar Observatory for Winds (GLOW), Proceedings of the 21st International Laser Radar Conference, Quebec City, Canada, July 8-12, 2002.

Gentry, G., S. Li, H. Chen, J. Comer, S. Mathur, and J. Dobler, Direct detection Doppler lidar wind measurements obtained during the 2002 International H2O Project (IHOP), 2nd Symposium on Lidar Atmospheric Applications, The 85th American Meteorological Society Annual Meeting (San Diego, CA), 2005.

Heckman, S. T., M. W. Maier, W. P. Roeder, J. B. Lorens, and B. F. Boyd, The operational use of a boundary layer profiler network at the Eastern Range and Kennedy Space Center. Preprints, 27th Conf. on Radar Meteorology, Vail, CO, American Meteorological Society, Boston, MA, 346–348, 1996.

Hildebrand, Peter H. and R. S. Sekhon, Objective determination of the noise level in Doppler spectra. J. Appl. Meteor., 13, 808-811, 1974.

Hollerman, I., Doppler RadarWind Profiles, Scientific Report, KNMI WR-2003-02 (Dutch Weather Service), 2003.

Ishii, S., Mizutani, K., Aoki, T., Sasano, M, Murayama, Y., Itabe, T., and Asai, K., Wind profiling with an eye-safe coherent doppler lidar system: comparison with radiosondes and VHF radar, J. Met. Soc. Japan, 83, 1041- 1056, 2005.

Jordan, J. R., R. J. Lataitis, and D. A. Carter, Removing ground and intermittent clutter contamination from wind profiler signals using wavelet transforms. J. Atmos. Oceanic Technol., 14, 1280–1297, 1997.

Klemp, J.B., and D.R. Durran, 1983: An upper boundary condition permitting internal gravity wave radiation in numerical mesoscale models. Mon. Wea. Rev., 111, 430-444.

Korb, C.L. , B.M. Gentry and S.X. Li, Edge technique wind measurements with high vertical resolution, Appl. Opt., 36, 5976-5983, 1997.

Krider, E. P., J. C. Willett, G. S. Peng, F.S. Simmons, G.W. Law, R. W. Seibold, Triggered Lightning Risk Assessment for Reusable Launch Vehicles at the Southwest Regional and Oklahoma Spaceports, Aerospace Report No. ATR-2006(5195)-1, 2006.

Larsen, M. F., Can a VHF Doppler radar provide synoptic wind data? A comparison of 30 days of radar and radiosonde data, Mon. Wea. Rev., 111, 2047–2057, 1983.

Leahy, Frank, An Analysis of the Automated Meteorological Profiling System Low Resolution Flight Element , AIAA-2004-908, 42nd AIAA Aerospace Sciences Meeting and Exhibit, Reno, Nevada, Jan. 5-8, 2004.

Luers, J. K., and C. D. MacArthur, Ultimate Wind Sensing Capabilities Of The Jimsphere And Other Rising Balloon Systems, NASA CR-2048, 101 pp., 1972.

Lumley, J. L. and H. A. Panofsky, The Structure of Atmospheric Turbulence, Monographs and Texts in Physics and Astronomy, Vol. 12, Wiley, 239, 1964.

May, P. T., and R. G. Strauch, Reducing the effect of ground clutter on wind profiler velocity measurements. J. Atmos. Oceanic Technol., 15, 579–586, 1998.

Menzeis R. T, and D. M. Tratt, Infrared Lidar sensitivity to cloud optical and geometrical properties; Implications for Earth-orbiting Doppler lidar, Proc. Seventh Cont. on Coherent Laser Radar Applications and Technology, Paris, France, CNES, CNRS, ESA, 107-110, 1993.

McGill, M. J. James and D. Spinhirne, Comparison of two direct-detection Doppler lidar techniques, Opt. Eng., 37, 2675–2686, 1998.

Merceret, F. J., Vertical resolution of the Kennedy Space Center 50-MHz wind profiler, J. Atmos. Oceanic Technol., 16, 1273 -1278, 1999.

Merritt, D., A statistical averaging method for wind profile Doppler spectra. J. Atmos. Oceanic Technol., 12, 985–995, 1995.

Michalakes, J., S. Chen, J. Dudhia, L. Hart, J. Klemp, J. Middlecoff, and W. Skamarock (2001): Development of a next generation regional weather research and forecast model" in Developments in Teracomputing: Proceedings of the Ninth ECMWF Workshop on the Use of High Performance Computing in Meteorology. Eds. Walter Zwieflhofer and Norbert Kreitz. World Scientific, Singapore. pp. 269-276.

Nastrom, G. D. and F. D. Eaton, Variations of winds and turbulence seen by the 50-MHz radar at White Sands Missile Range, New Mexico. J. Appl. Meteor., 34, 2135-2148, 1995.

Petheram, J. C., G. Frohbeiter, and A.Rosenberg, Carbon dioxide Doppler lidar wind sensor on a space station polar platform, Appl. Opt., 28, 834–839, 1989.

Pielke R. A. and R. P. Pearce, Mesoscale Modeling of the Atmosphere, Meteorological Monograph Series, Vol. 25, No. 47, ISBN 1-878220-15-2, 167 pp., 1994.

Rocadenbosch, F., Lidar – wind, Raman and other sensing, <u>Encyclopedia of Optical Engineering</u>, Vol. 2, R. Driggers, Ed., 114-127, Marcel Dekker, 2003.

Rothermel, J., D. A. Bowdle, J. M. Vaughan, and M. J. Post, Evidence of a tropospheric aerosol background backscatter mode. <u>Appl. Opt., 28</u>, 1040-1042, 1989.

Schumann, R. , Taylor, G. E.; Smith, S. A.; Wilfong, T. L. Application of 50 MHz Doppler radar wind profiler to launch operations at Kennedy Space Center and Cape Canaveral Air Station, NASA-CR-201409, 1994.

Schumann, R. S., G. E. Taylor, F. J. Merceret, T. L. Wilfong, Performance Characteristics of the Kennedy Space Center 50-MHz Doppler Radar, Wind Profiler Using the Median Filter/First-Guess Data Reduction Algorithm, <u>J. Atmos. Oceanic Technol.,</u> 532-549, 1999.

Smith, S. A. 1997: Mesoscale wind variability and profiler precision. Manuscript submitted to JTEC.

Strauch, R. G., D. A. Merritt, K. P. Moran, K. B. Earnshaw, and D. C. Welsh,: The Colorado wind profiling network. <u>J. Atmos. Oceanic Technol., 1</u>, 37–49, 1984.

Strauch, R. G., B. L. Weber, A. S. Frisch, C. G. Little, D. A. Merritt, K. P. Moran, and D.C. Welsh, The precision and relative accuracy of profiler wind measurements. <u>J. Atmos. Oceanic Technol., 4</u>, 563-571,1987.

van de Kamp D.W. 1988, Profiler training manual #2: quality control of wind profiler data. Report prepared for the National Weather Service Office of Meteorology by NOAA/WPL, Boulder, CO.

Wandinger, U., Introduction to lidar, in <u>Lidar - Range-Resolved Optical Remote Sensing of the Atmosphere,</u> C. Weitkamp (Ed.). Springer, New York, 2005.

Weber, B. L. and Wuertz, <u>Quality Control Algorithm For Profiler Measurements Of Winds And RASS Temperatures</u>, NOAA Tech. Memo. ERL WPL-212, 32 pp., 1991.

Weber, B. L., D. B. Wuertz, and D.C. Welsh, Quality controls for profiler measurements of winds and RASS temperatures. <u>J. Atmos. Oceanic Technol., 10</u>, 452-464, 1993.

Werner, C., Doppler lidar, in Lidar - Range-Resolved Optical Remote Sensing of the Atmosphere, C. Weitkamp (Ed.) Springer, New York, 2005.

Wilczak J.M, R. G. Strauch, F. M. Ralph, B. L. Weber, D. A. Merritt, J. R. Jordan, D. E. Wolfe, L. K. Lewis, D. B. Wuertz, J. E. Gaynor, S. A. McLaughlin, R. R. Rogers, A. C. Riddle, and T. S. Dye, Contamination of wind profiler data by migrating birds: Characteristics of corrupted data and potential solutions, <u>J. Atmos. Oceanic Technol.</u>, 12, 449–467, 1995.

Wilfong, T. L., R. L. Creasey and S. A. Smith, Wind persistence from 2-18 km using a wind profiler. *Paper AIAA-93-0854*, AIAA 31st Aerospace Sciences Meeting and Exhibit (Jan 1993), 1993a.

Wilfong, T. L., S. A. Smith, and R. L. Creasey, High temporal resolution velocity estimates from a wind profiler. J. Spacecraft and Rockets, 30, 348-354, 1993b.

Wilfong, T. L., S. A. Smith, and C. L. Crosiar, Characteristics of high-resolution wind profiler derived from radar-tracked jimspheres and the rose processing program. J. Atmos. Ocean. Tech., 14, 318-325, 1997.

WRIH, Western Range Instrumentation Handbook, CDRL Sequence Number B533 DI-MISC-80711A2/T, Prepared for 30th Space Wing, Vandenberg AFB, 2007.

Wuertz, D. B., B. L. Weber, R. G. Strauch, A. S. Frisch, C. G. Little, D. A. Merritt, K. P. Moran, and D. C. Welsh, Effects of precipitation on UHF wind profiler measurements. J. Atmos. Oceanic Technol., 5, 450–465, 1988.

Wuertz, D. B., and B. L. Weber, Editing Wind Profiler Measurements, NOAA Wave Propagation Laboratory Tech. Rep. ERL438-WPL 92, 62 pp., 1989.

Abbreviations and Acronyms

AC	Air Conditioning
AFWA	Air Force Weather Agency
AGL	Above ground level
AMPS	Automated Meteorological Profiling System
CCAFS	Cape Canaveral Air Force Station
CSLAA	Commercial Space Launch Amendments Act
CW	Continuous Wave
DGPS	Differential GPS
DRWP	Doppler Radar Wind Profiler
ER	Eastern Range
FE	Flight Element
GE	Ground Element
GLOW	Goddard Lidar Observatory for Wind
GPS	Global Positioning System
HRFE	High Resolution Flight Element (AMPS)
IHOP	International H_2O Project
IR	Infrared
KSC	Kennedy Space Center
LIDAR	Light Detection and Ranging
LO	Local Oscillator
LRFE	Low Resolution Flight Element (AMPS)
MFFG	Median Filter First Guess
MM5	Mesoscale Model 5
NASA	National Aeronautics and Space Administration
NCAR	National Center for Atmospheric Research
Nd:YAG	Neodymium-Doped Yttrium Aluminum Garnet
NOAA	National Oceanic and Atmospheric Administration
NWP	Numerical Weather Prediction
OPO	Optical Parametric Oscillator
PMT	Photon-counting Photomultiplier Tube
PRD	Program Requirements Document
QC	Quality Control
RASS	Radio Acoustic Sounding System
RF	Radio Frequency
RFI	Radio Frequency Interference
RLV	Reusable Launch Vehicle
RMS	Root Mean Square
SNR	Signal-to-Noise Ratio
SPS	Signal Processing Subsystem
SSP	Space Shuttle Program
UHF	Ultra-High Frequency
UV	Ultraviolet (radiation)
VHF	Very High Frequency (radiation)
WR	Western Range
WRF	Weather Research and Forecasting (model)

Appendix A. Profiles of MM5 Bias and Precision for
Wind Speed and Direction

Figures A-1 – A-8 show plots of verification statistics for both MM5 for various sites in the southwestern United States for the period from 1 January to 31 March 2009. The plots were provided by Mr. Robert Craig [Air Force Weather Agency, Offutt AFB, NB]. The data are the root-mean-square errors and biases for 6, 18, 20, and 42 hour forecasts for various sites. The data are given in knots (1 knot = 0.5144 m/s). Data are for wind speed and direction.
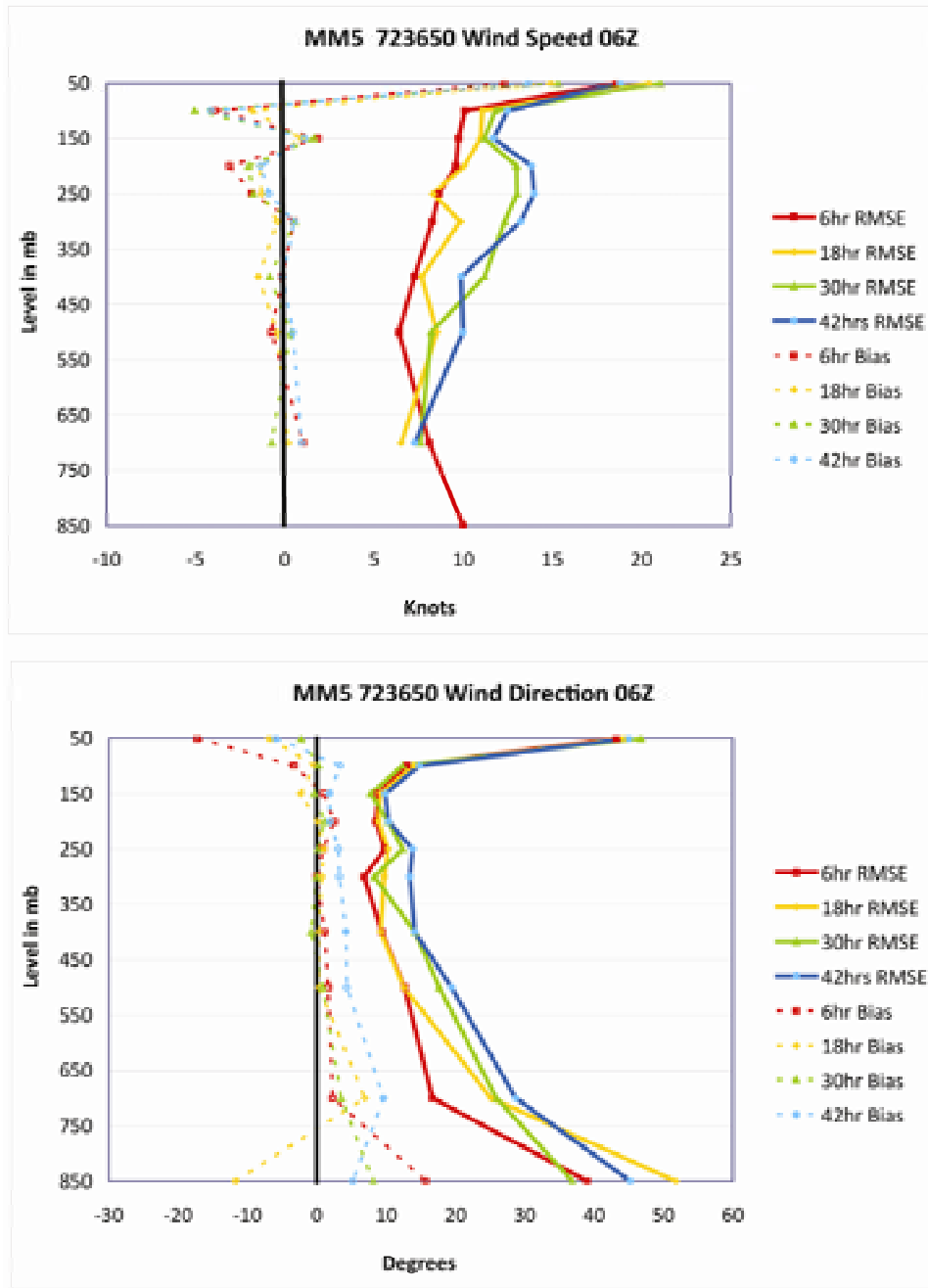
Figure A-1. Vertical Profiles of Bias and RMS Error of Wind Speed (Upper) and Direction (Lower) for the MM5 for Albuquerque, NM.

MM5 723630 Wind Speed 06Z

MM5 723630 Wind Direction 06Z
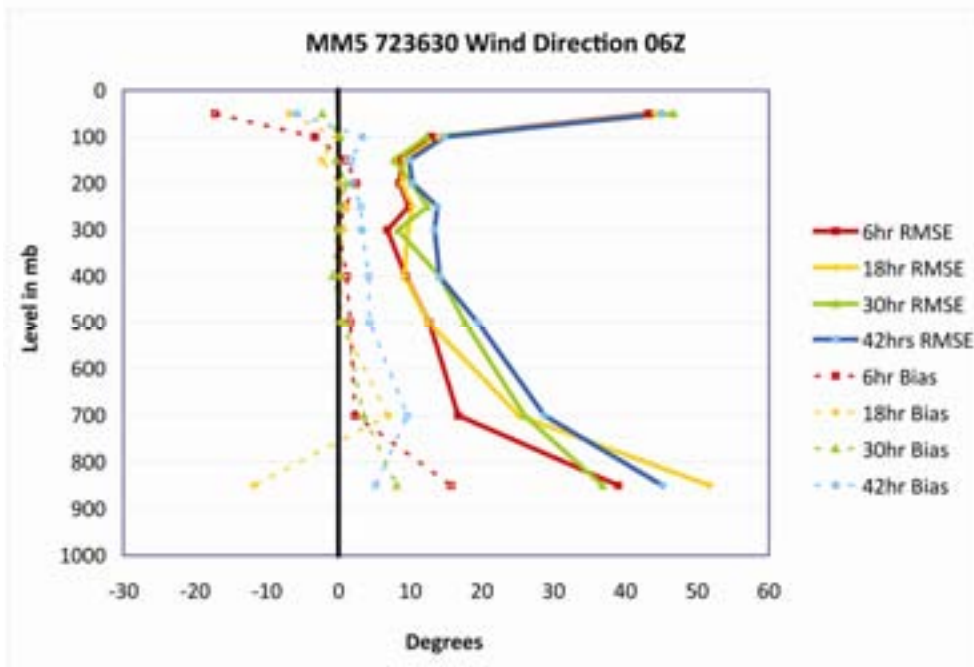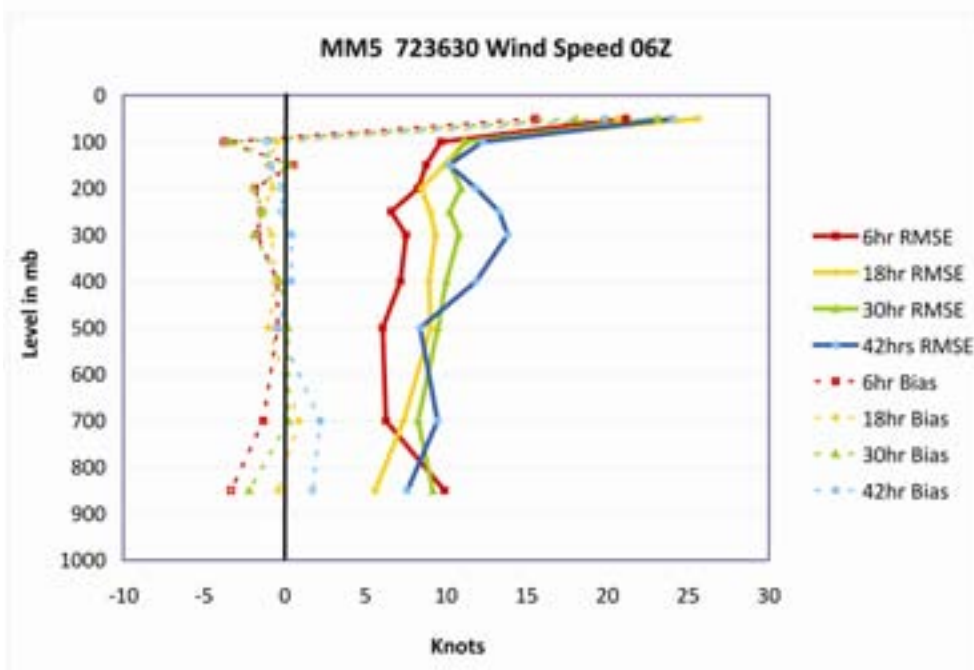
Figure A-2. Same as Figure A-1 Except for Amarillo, TX.

MM5 722490 Wind Speed 06Z

MM5 722490 Wind Direction 06Z
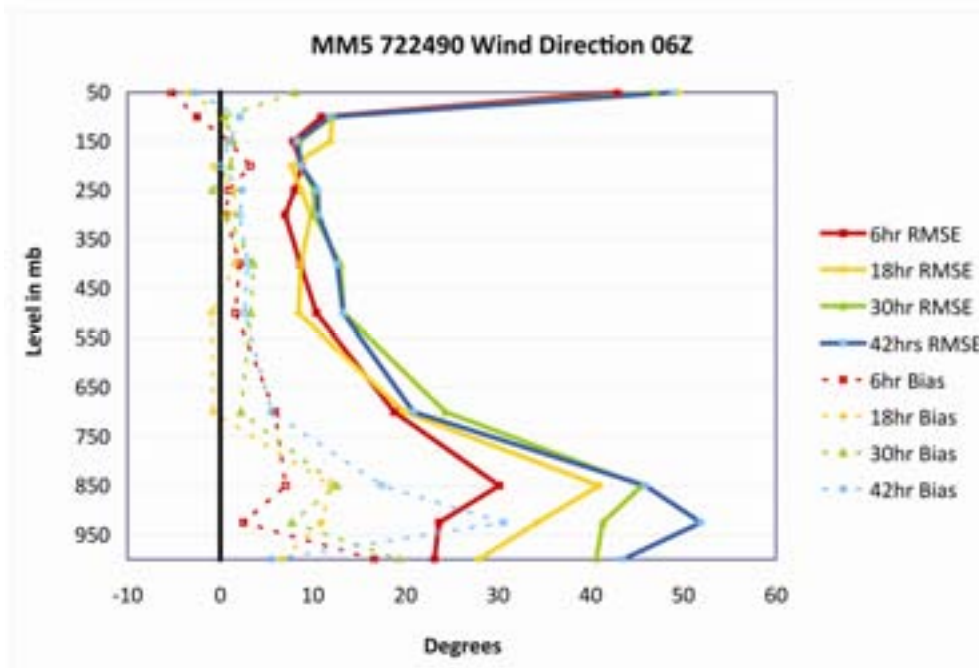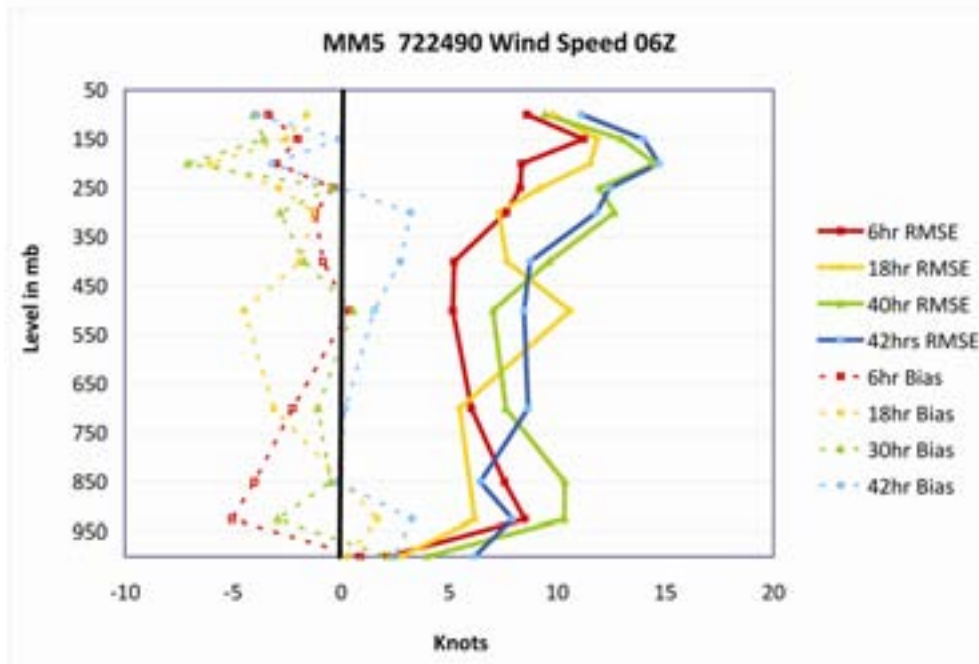
Figure A-3. Same as Figure A-1 Except for Dallas, TX.
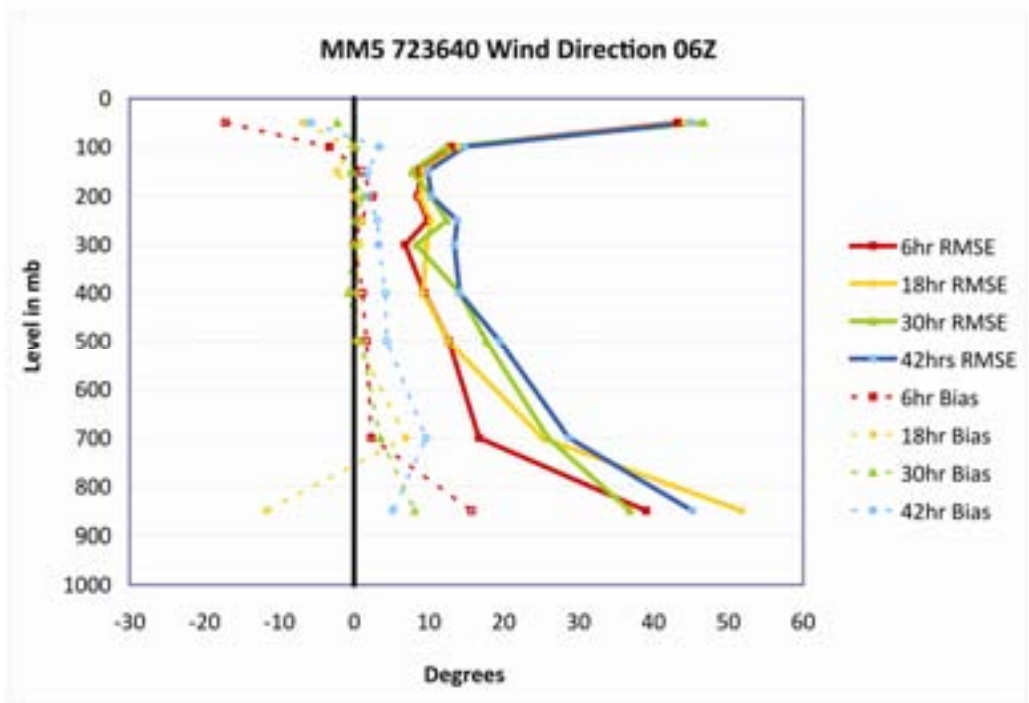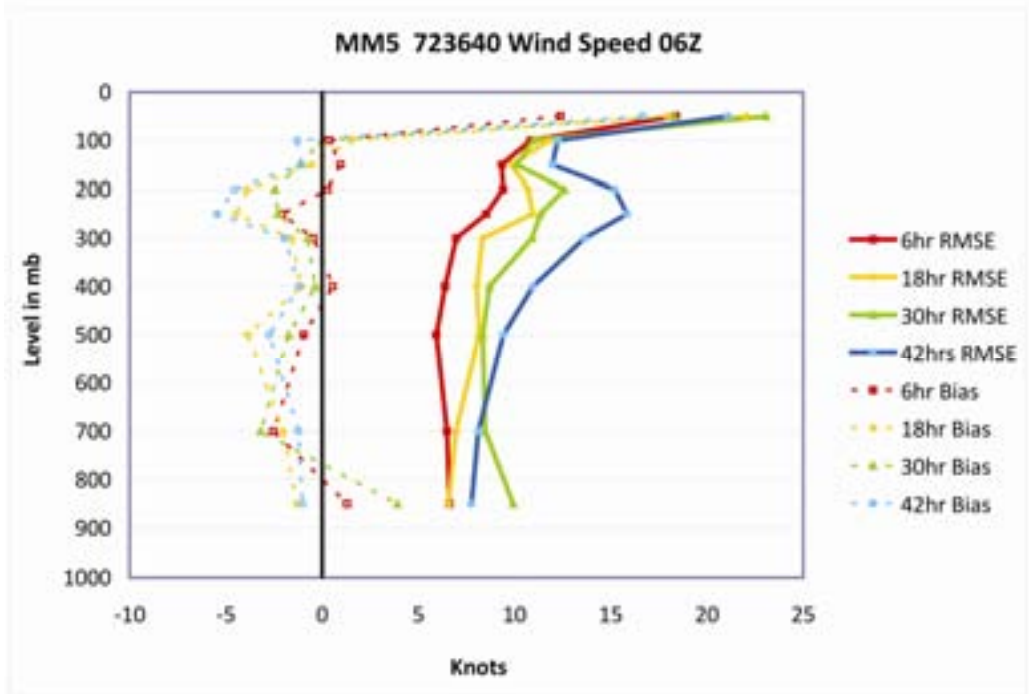
Figure A-4. Same as Figure A-1 Except for El Paso, TX.
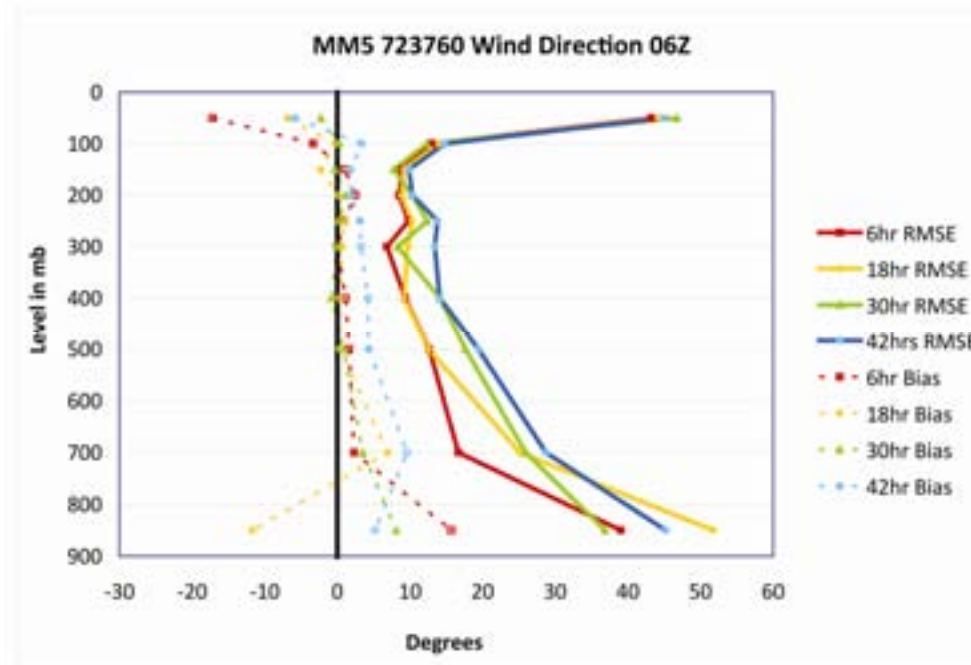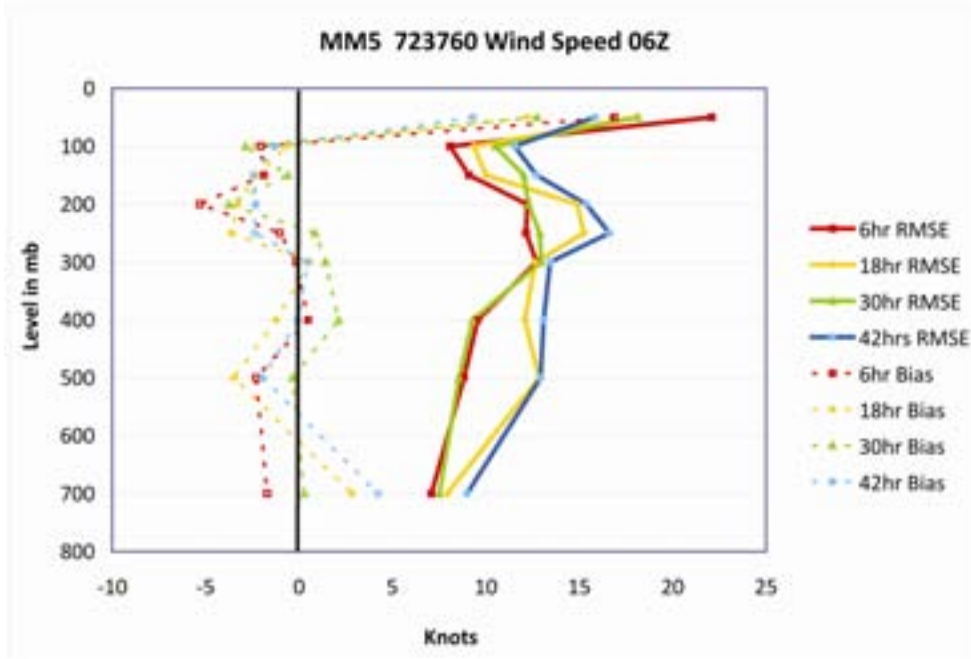
Figure A-5. Same as Figure A-1 Except for Flagstaff, AZ.
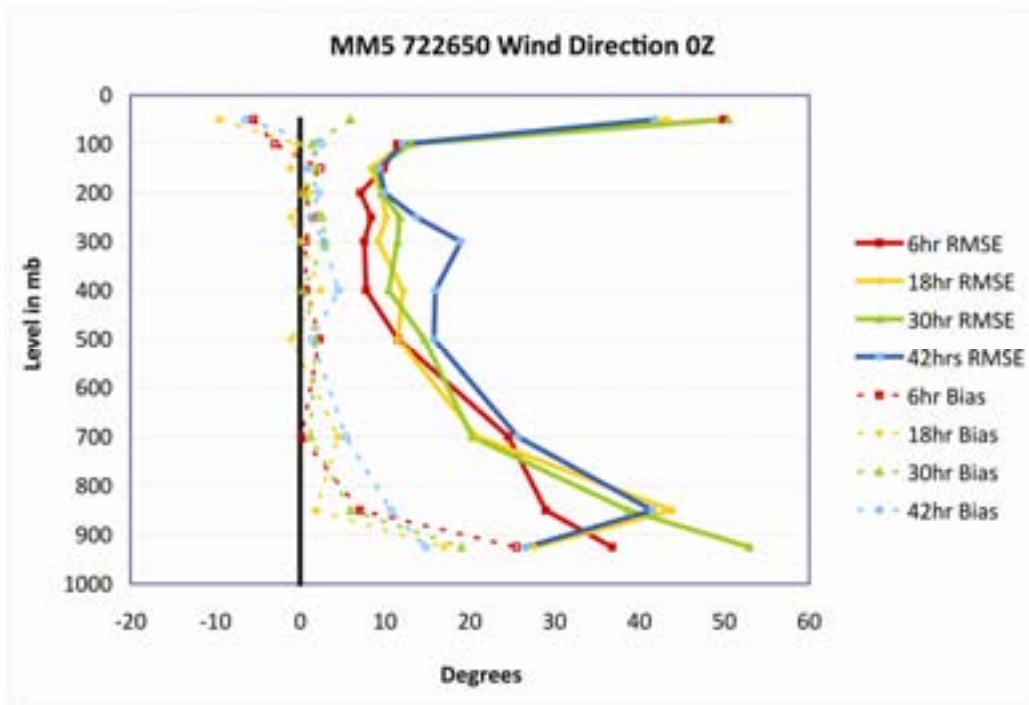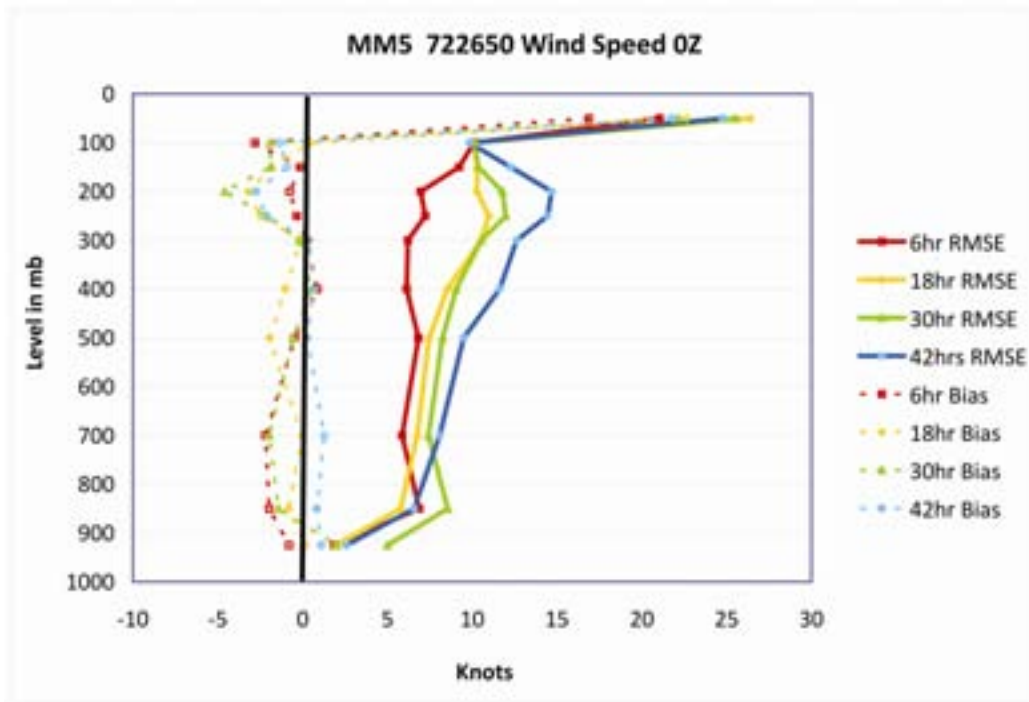
Figure A-6. Same as Figure A-1 Except for Midland, TX.
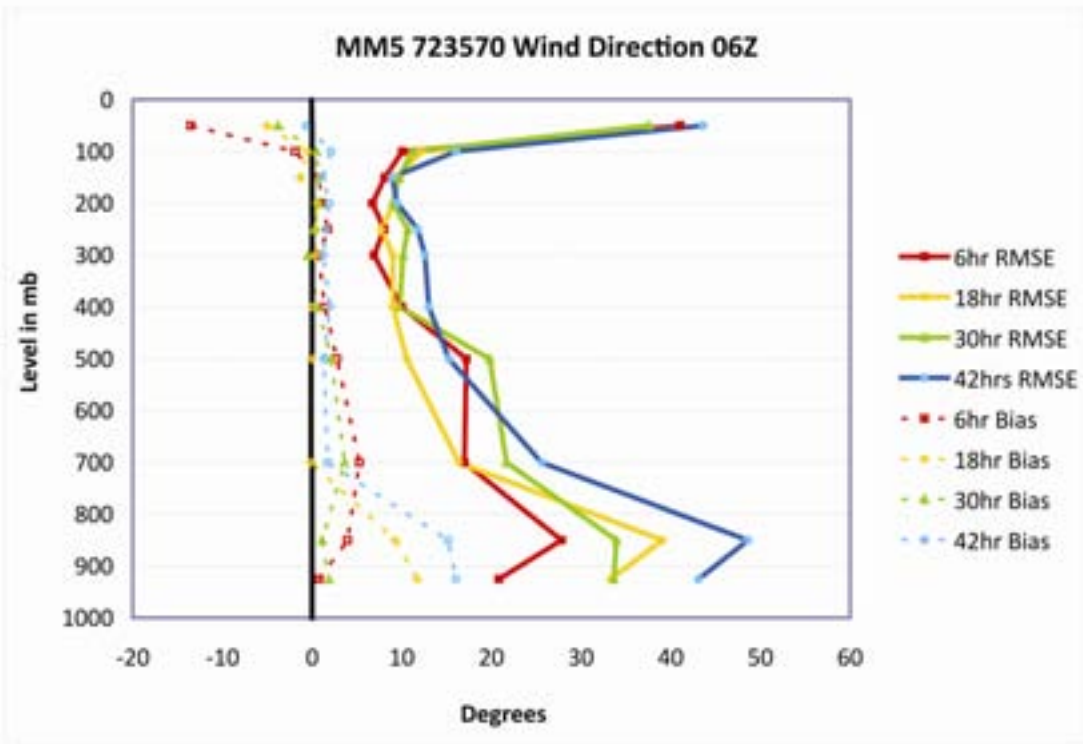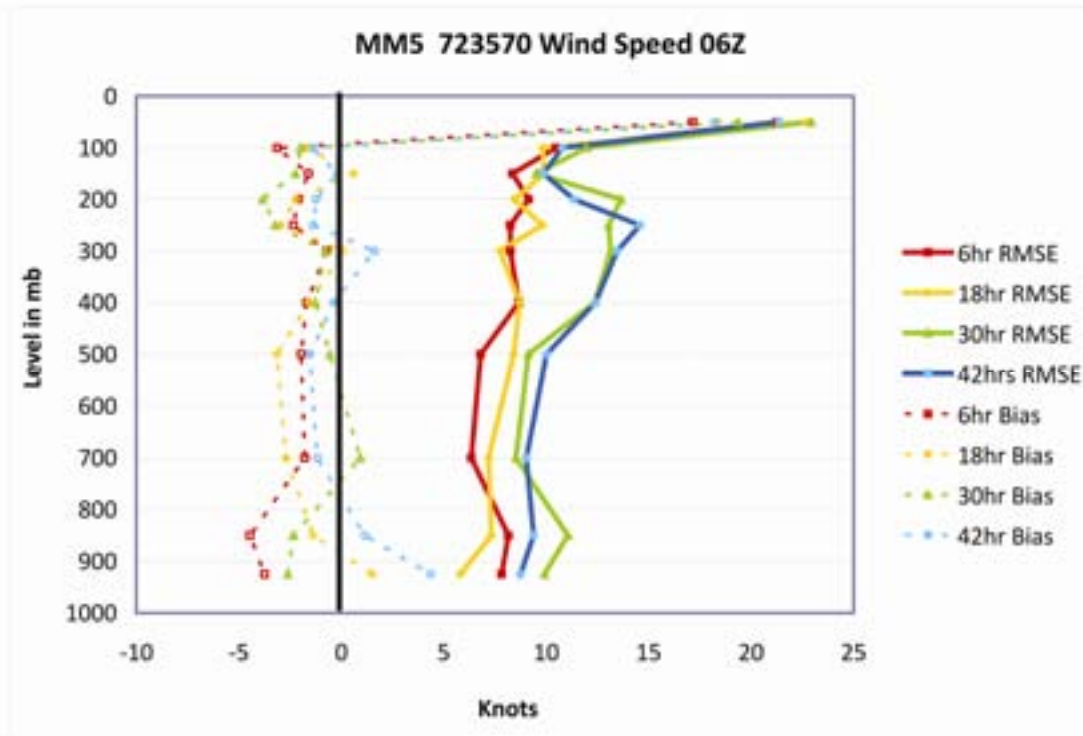
Figure A-7. Same as Figure A-1 Except for Oklahoma City, OK.
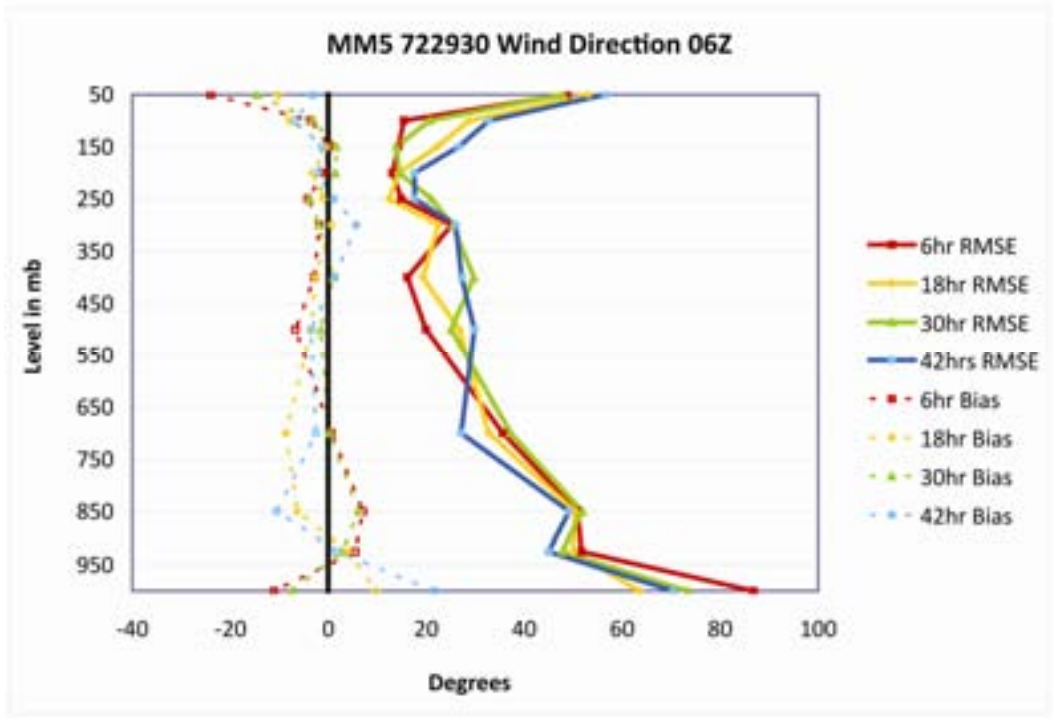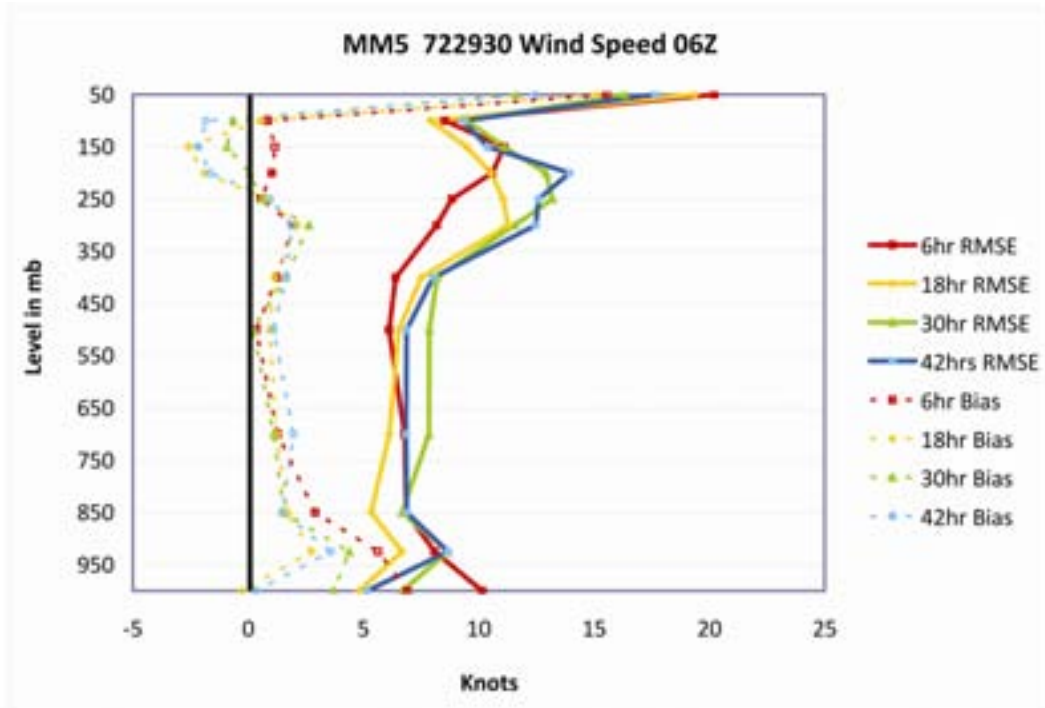
Figure A-8. Same as Figure A-1 Except for San Diego, CA.

Appendix B. Profiles of WRF Bias and Precision for Wind Speed and Direction

Figures B-1 – B-8 show plots of verification statistics for both MM5 for various sites in the southwestern United States for the period from 1 January to 31 March 2009. The plots were provided by Mr. Robert Craig [Air Force Weather Agency, Offutt AFB, NB]. The data are the root-mean-square errors and biases for 6, 18, 20, and 42 hour forecasts for various sites. The data are given in knots (1 knot = 0.5144 m/s). Data are for wind speed and direction. Note that 0 hr refers to the assimilation errors, that is, the errors in the initial field.
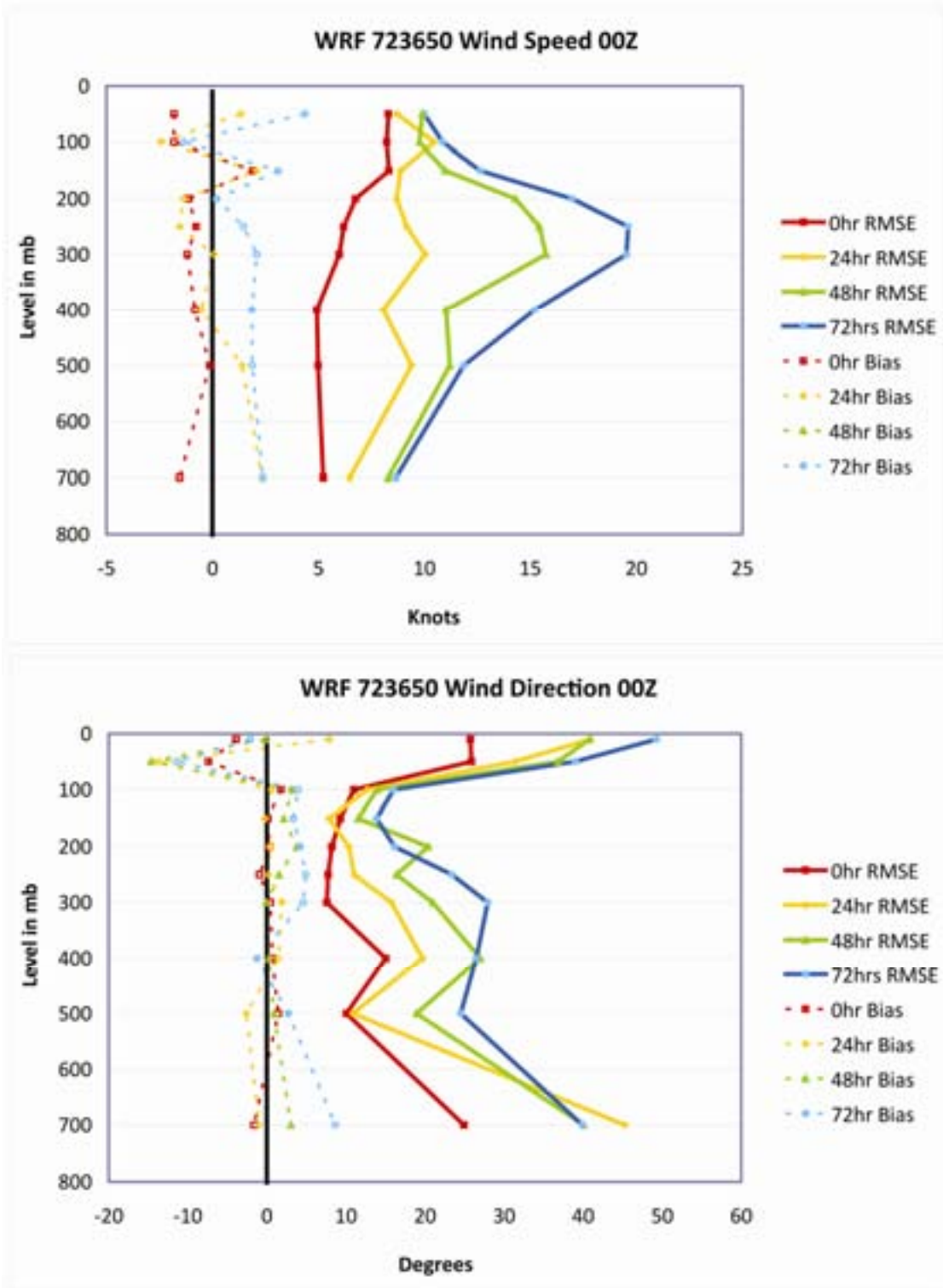
Figure B-1. Vertical Profiles of Bias and RMS Error of Wind Speed (Upper) and Direction (Lower) for the WRF Model for Albuquerque, NM.
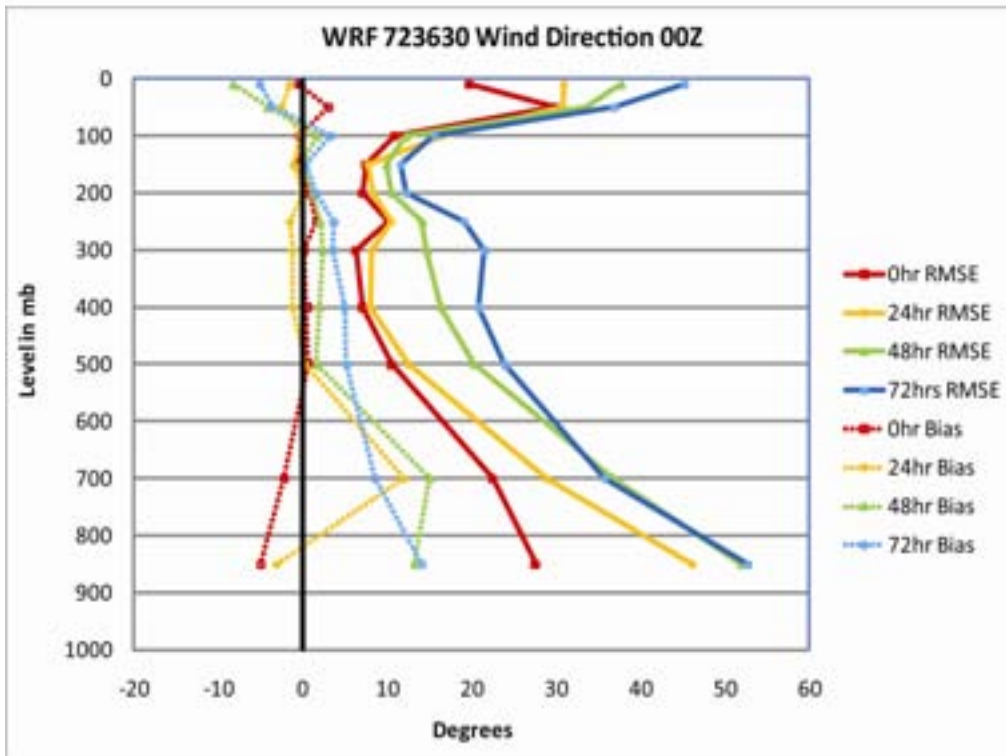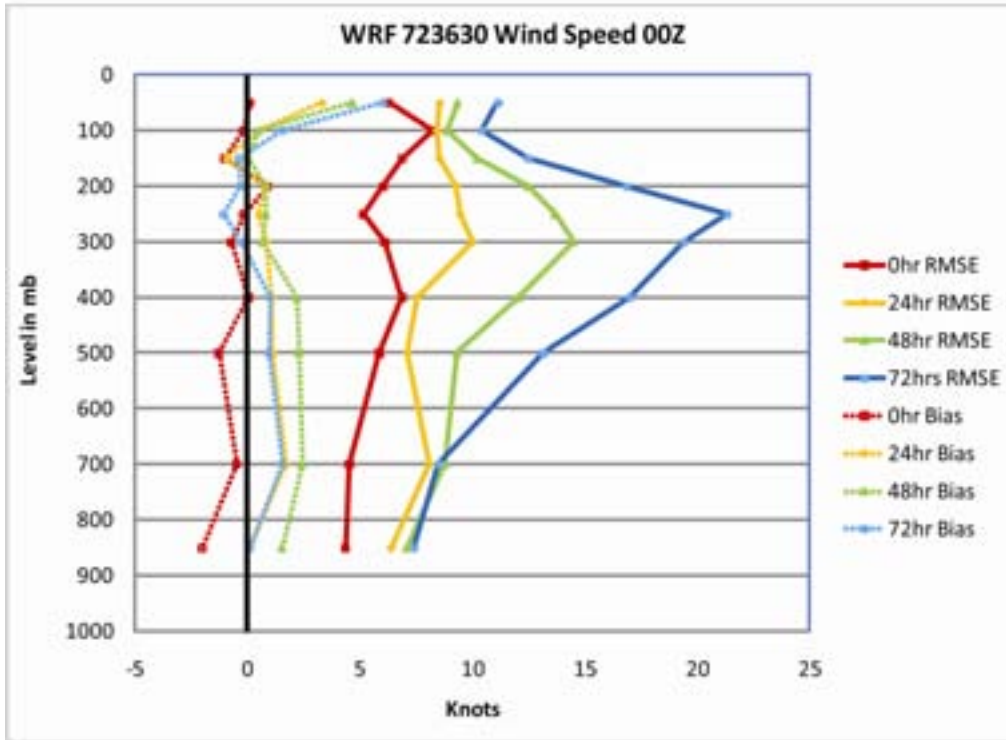
Figure B-2. Same as Figure B-1 Except for Amarillo, TX.

WRF 722490 Wind Speed 00Z

WRF 722490 Wind Direction 00Z
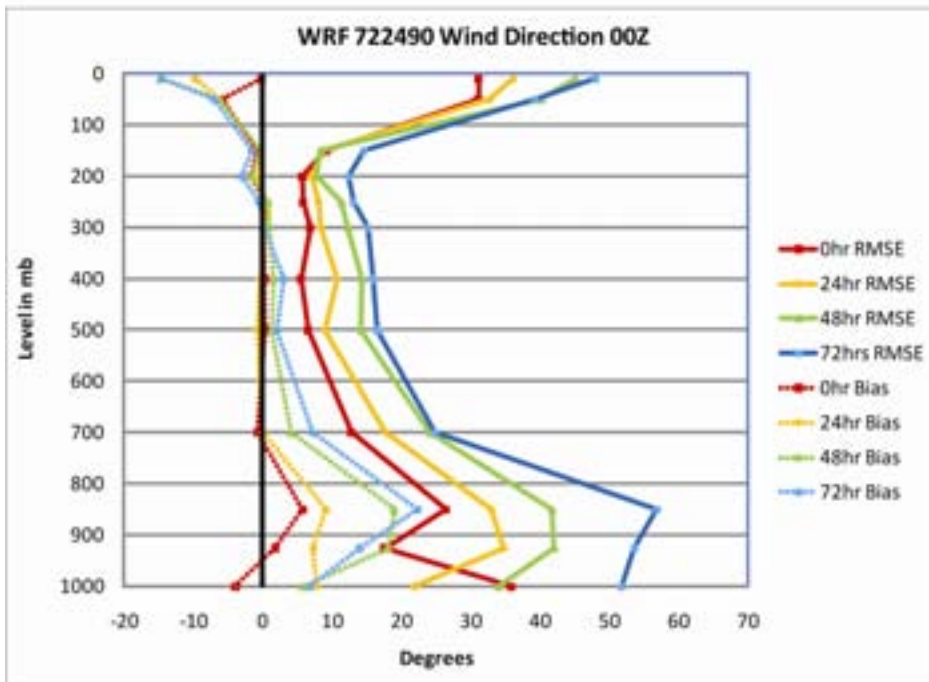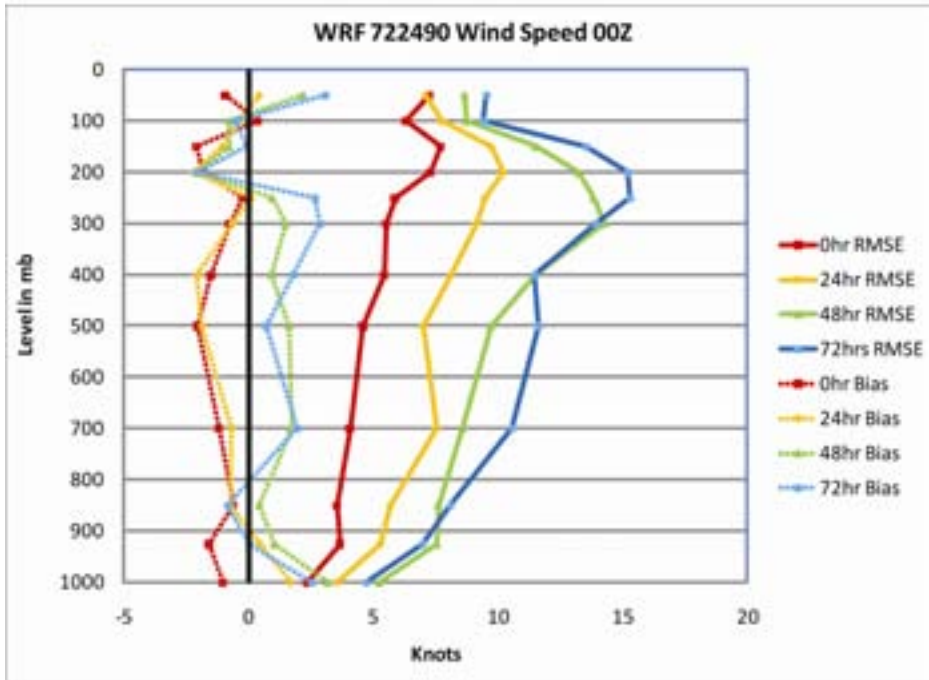
Figure B-3. Same as Figure B-1 Except for Dallas, TX.
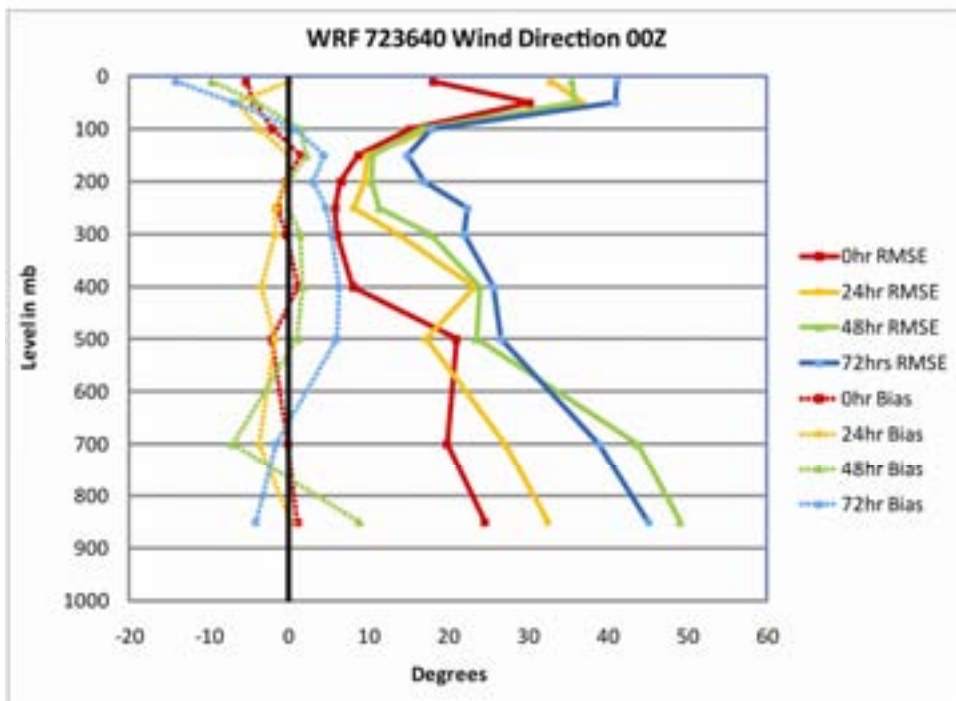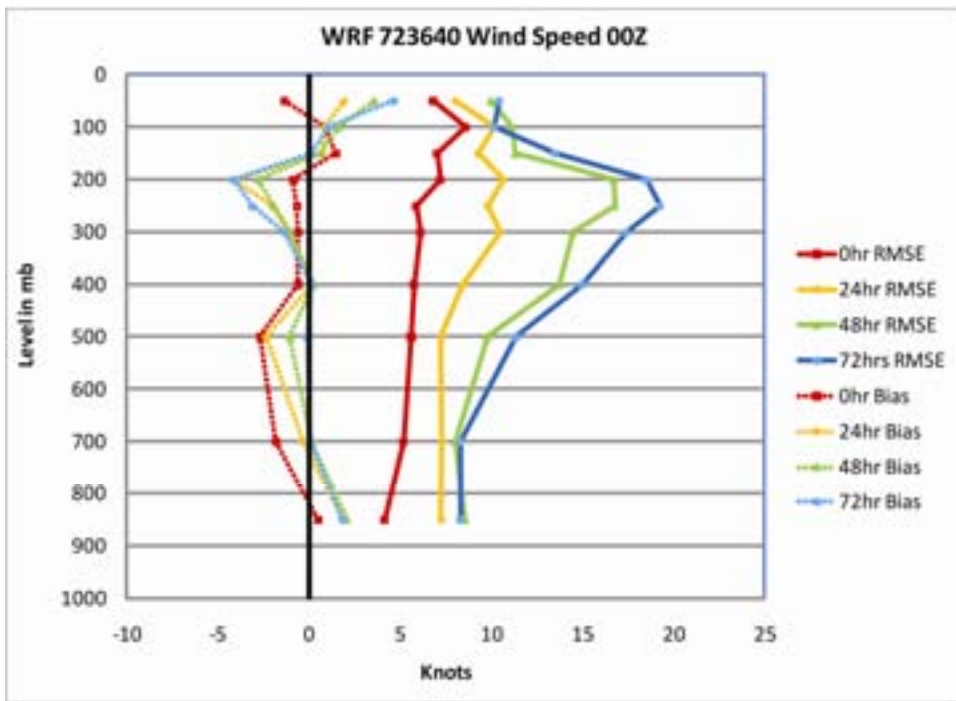
Figure B-4. Same as Figure B-1 Except for El Paso, TX.
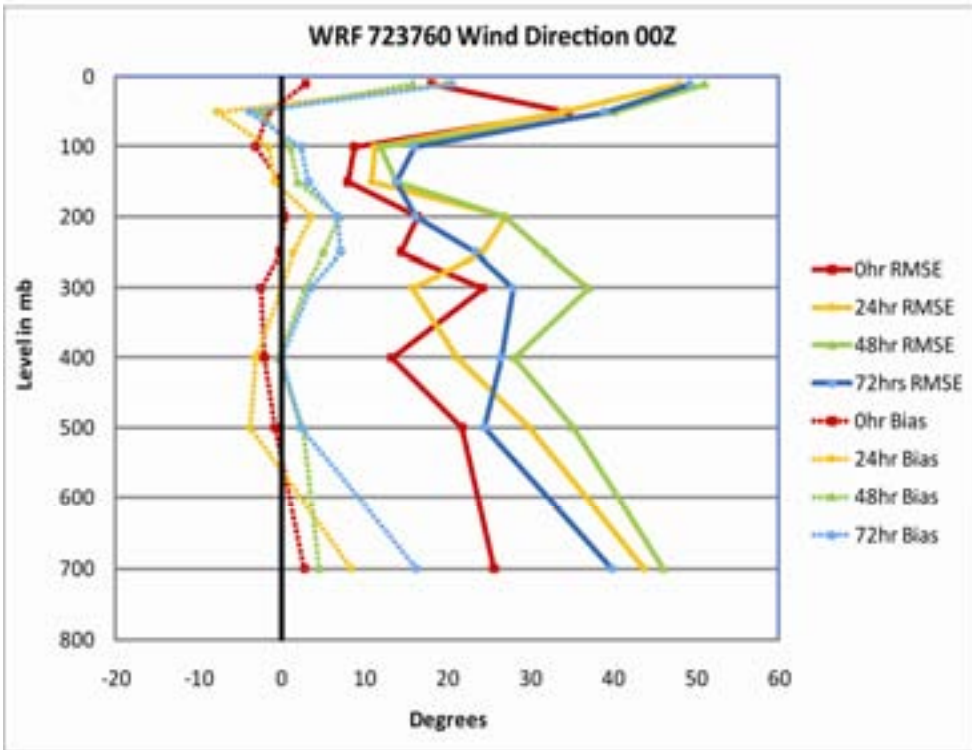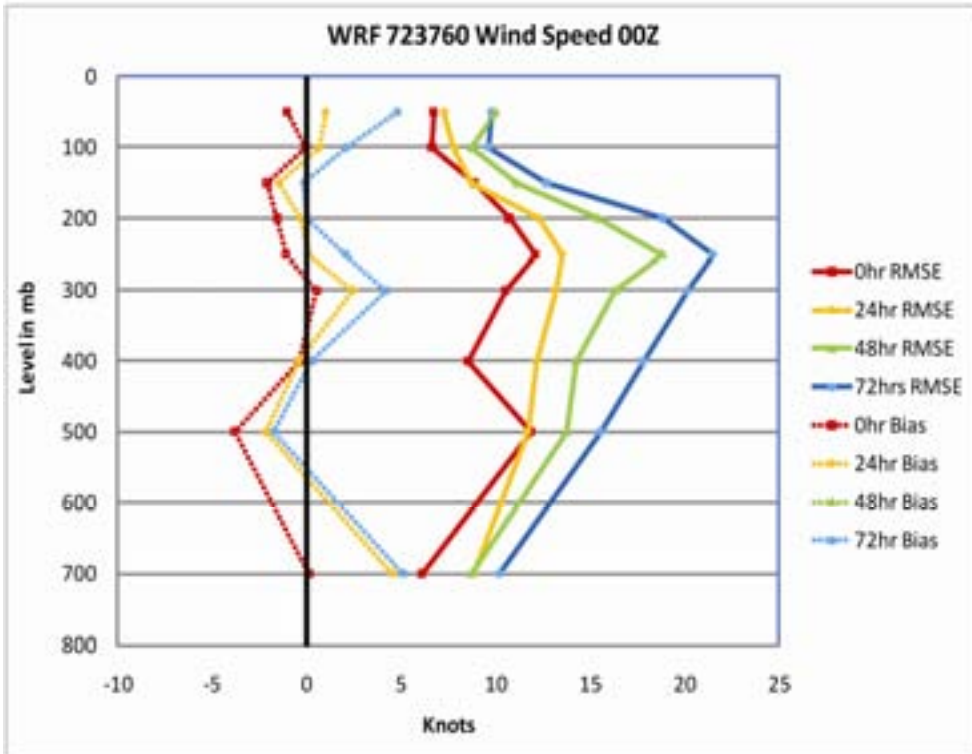
Figure B-5. Same as Figure B-1 Except for Flagstaff, AZ.
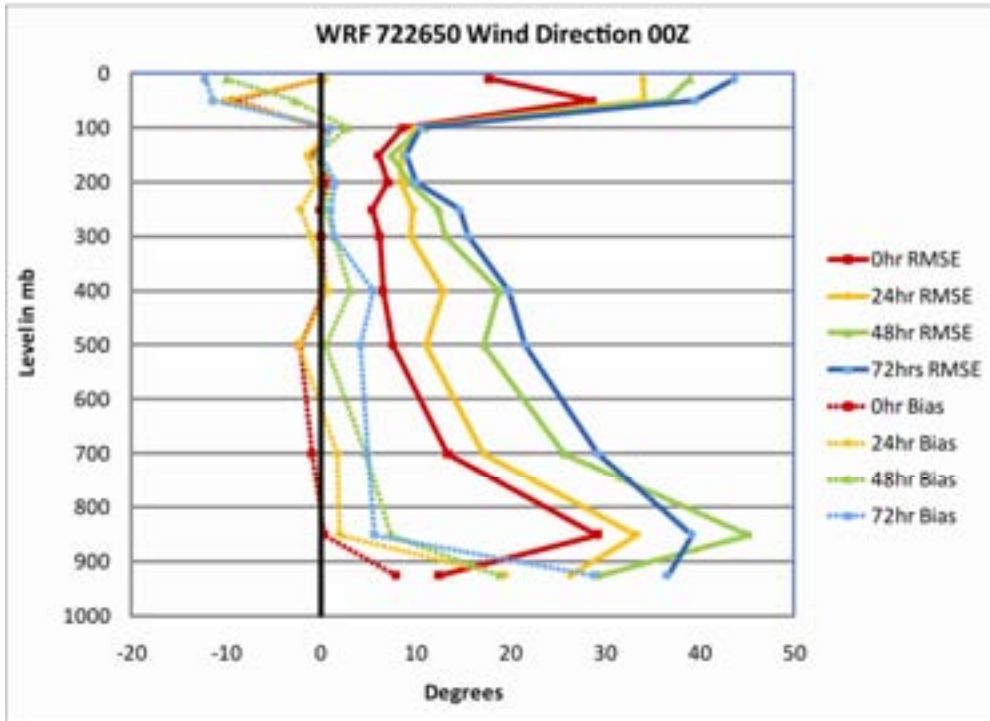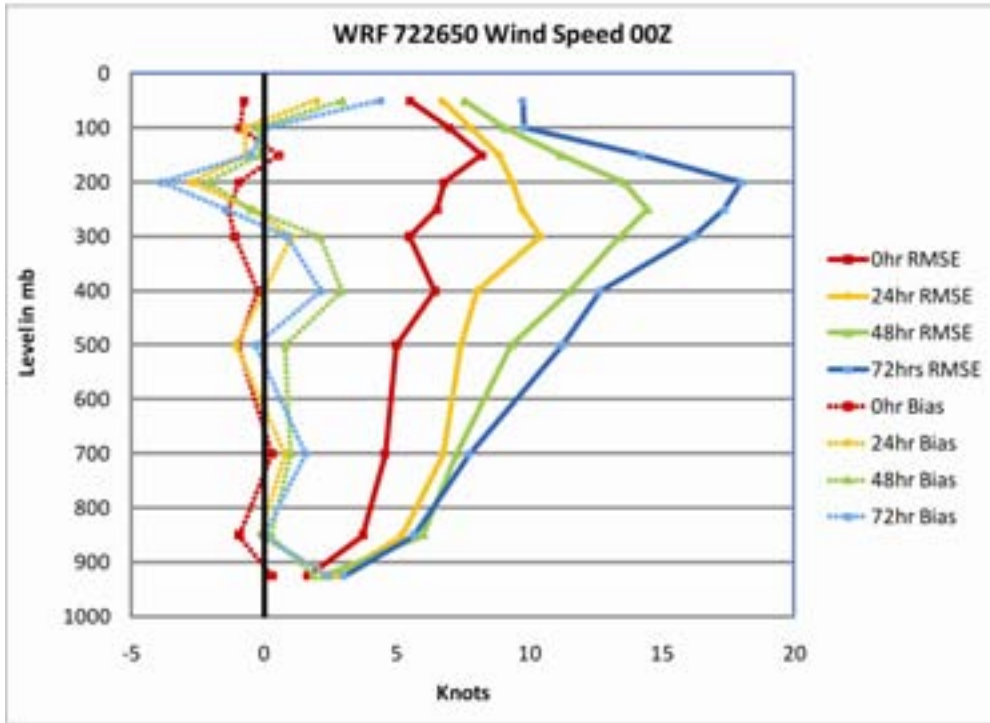
Figure B-6. Same as Figure B-1 Except for Midland, TX.
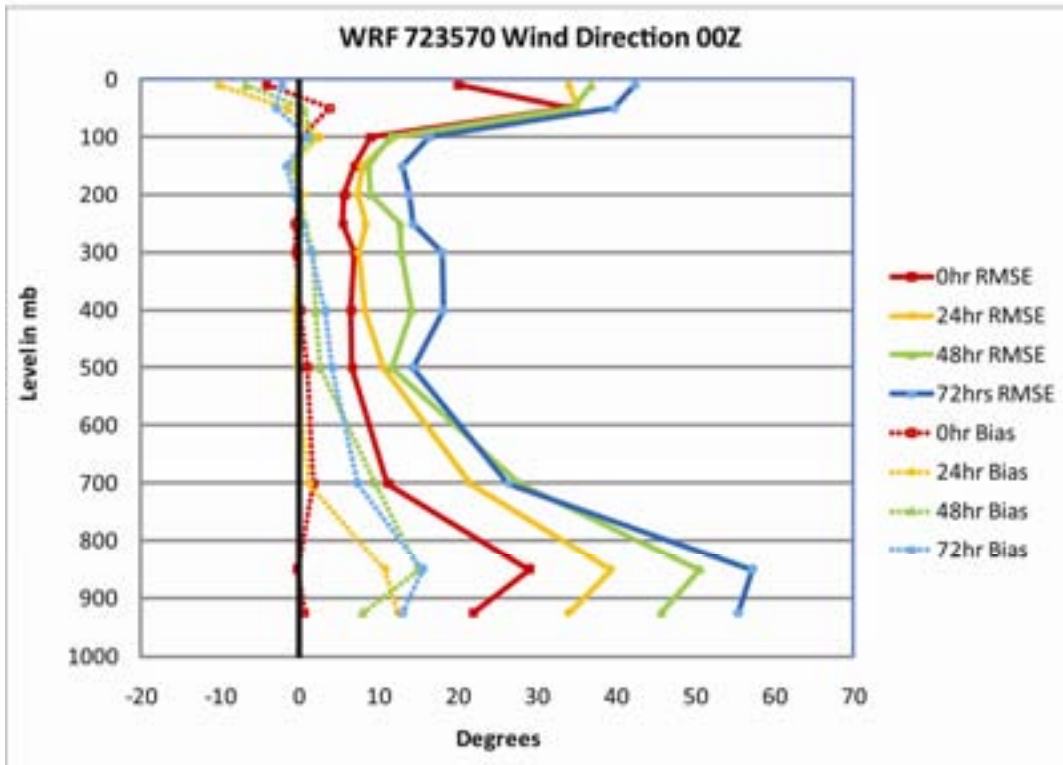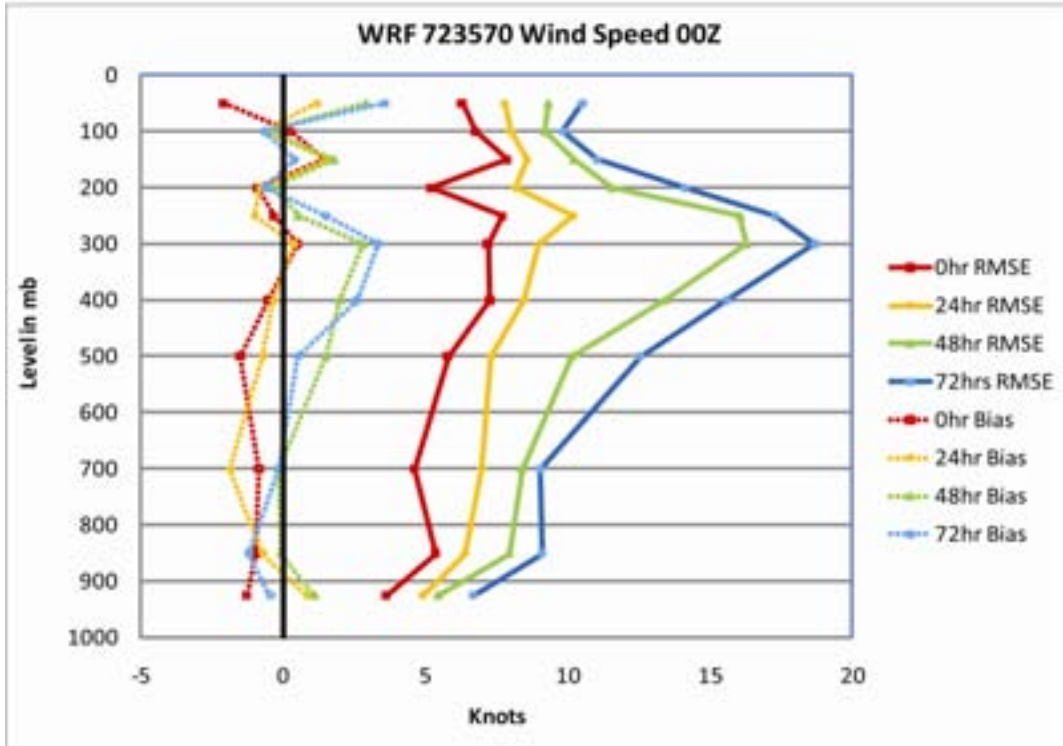
Figure B-7. Same as Figure B-1 Except for Oklahoma City, OK.
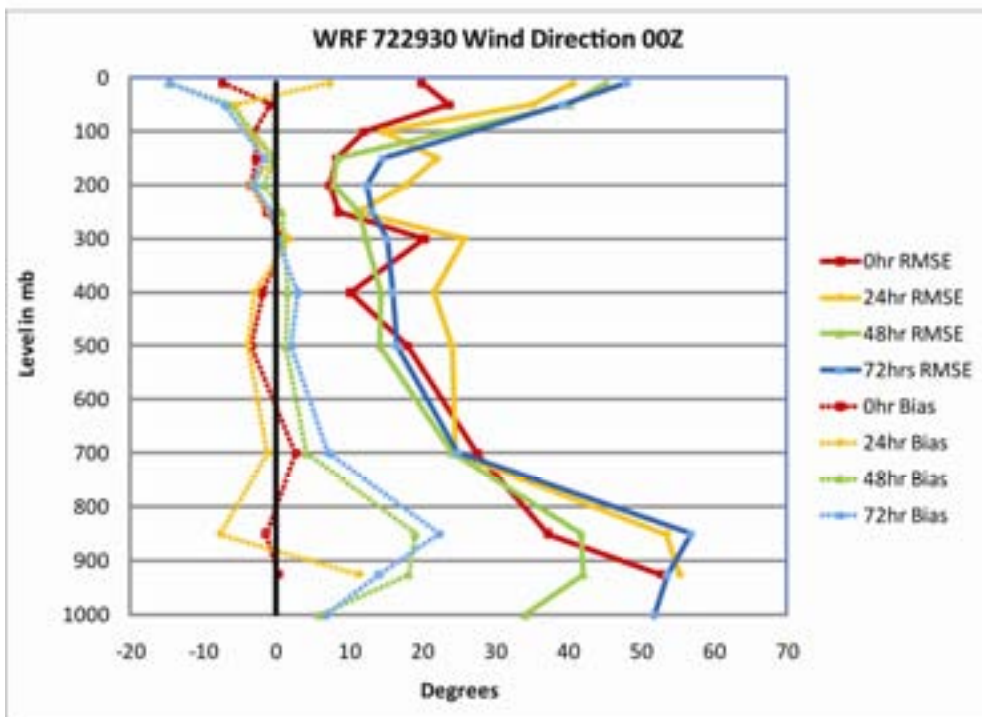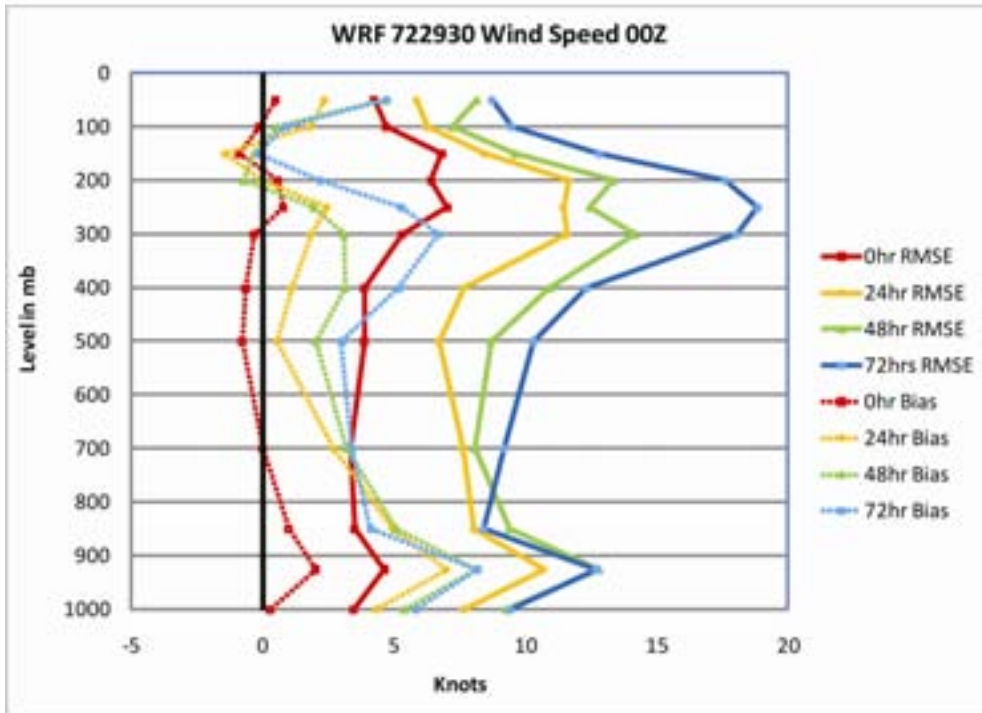
Figure B-8. Same as Figure B-1 Except for San Diego, CA.